European Journal of Chemistry

Check for updates

View Journal Online
View Article Online

Design and synthesis of new coumarin-1,2,3-triazole hybrids as new antidiabetic agents: *In vitro* α-amylase, α-glucosidase inhibition, anti-inflammatory, and docking study

Vinayaka Chandrappa Barangi [1,2], Lokesh Anand Shastri [1,*], Prakasha Kothathi Chowdegowda [2], Rohini Sangappanavar [2], Karthik Inamdar [2], Nagarjuna Prakash Dalbanjan [3], Delicia Avilla Barretto [4], and Vinay Sunagar [5]

[1] *Department of Chemistry, Karnatak University, Dharwad-580003, Karnataka, India*
[2] *Department of Chemistry, Karnatak Lingayat Education, Parappa Channappa Jabin Science College, Hubballi-580031, Karnataka, India*
[3] *Department of Biochemistry, Karnatak University, Dharwad, Karnataka 580003, India*
[4] *School of Chemical Sciences, Goa University, Taleigao Plateau-403206, Panaji, Goa, India*
[5] *Department of Chemistry, Govindram Seksaria Science College, Belagavi, Karnataka 590006 India*

* *Corresponding author at: Department of Chemistry, Karnatak University, Dharwad-580003, Karnataka, India.*
e-mail: drlashastri@kud.ac.in (L.A. Shastri).

RESEARCH ARTICLE

10.5155/eurjchem.15.3.205-219.2541

Received: 29 February 2024
Received in revised form: 24 April 2024
Accepted: 28 June 2024
Published online: 30 September 2024
Printed: 30 September 2024

KEYWORDS

Diabetes
Triazoles
Coumarins
Inflammation
alpha-Amylase
alpha-Glucosidase

ABSTRACT

The current study focuses on the synthesis of coumarin-triazole hybrids (7i-t) starting from 4-hydroxy benzaldehyde or 4-hydroxyacetophenone (1a-b) and propargyl bromide. On the other hand, coumarin derivatives (5c-h) were prepared by *Pechmann* cyclization and treated with sodium azide to give the corresponding 3-azido methyl coumarins (6c-h). Finally, 1,3-dipolar cycloaddition between compounds 6c-h and terminal alkyne 2a-b produces coumarin-triazole hybrids (7i-t) utilizing click chemistry approaches that are high yielding, wide in scope and simple to perform. The structural proofs of the newly synthesized coumarin-triazole hybrids (7i-t) are proved by various spectroscopic techniques, including IR, ^{1}H NMR, ^{13}C NMR, and LC-MS. The synthesized new coumarin triazole hybrids (7i-t) were explored for their antihyperglycemic potential and therefore evaluated for α-glucosidase and α-amylase inhibitory activities along with anti-inflammatory. The results suggest that among the series, compound 7l showed excellent activity with an IC_{50} value of 0.67±0.014 mg/mL and 0.72±0.012 mg/mL for α-amylase, and α-glucosidase inhibitory potential while compound 7o showed promising anti-inflammatory activity with IC_{50} value of 0.54±0.003 mg/mL. To support the above findings, molecular docking studies were performed, which confirmed the interaction of the synthesized molecules 7i-t with an effective binding energy of -9.0 to -10.6 kcal/mol at the active site of the enzyme human pancreatic α-amylase (PDB ID: 1B2Y). Therefore, these scaffolds have the potential to function as lead candidates for antidiabetic and anti-inflammatory activities.

Cite this: *Eur. J. Chem.* **2024**, *15(3)*, 205-219 **Journal website**: www.eurjchem.com

1. Introduction

Chronic hyperglycemia is the hallmark of a group of metabolic diseases known as diabetes and is caused by abnormalities in insulin secretion. A person with diabetes has a body that cannot create enough insulin or will not respond to it. Based on how the body reacts to insulin and vice versa, diabetes is divided into two types. Type 1 diabetes, an autoimmune reaction in which the body restricts insulin production and requires daily insulin doses for proper functioning and survival; and type 2 diabetes, also known as hyperglycemia, in which high blood sugar occurs due to inadequate insulin secretion or insulin resistance in the body. Type 2 diabetes affects 90-95% of diabetics and poses a global health risk. This metabolic disorder leads to many complications including cardiovascular [1], neuropathy [2], retinopathy [3], and nephropathy [4] diseases.

Biologically, carbohydrates are the main source of energy that is subsequently broken down into oligosaccharides, disaccharides, and simpler glucose by endocrine and exocrine enzymes present in our body, like α-amylase secreted by the pancreas, which breaks polysaccharides into oligosaccharides and disaccharides. α-Glucosidase enzyme secreted by the small intestine breaks it further into glucose, which ultimately increases the blood sugar level, which is further assimilated by cells in response to insulin production by the pancreas. This diabetes can be controlled by reducing postprandial hyperglycemia [5] by delaying glucose absorption of glucose through the inhibition of enzymes such as α-amylase and α-glucosidase [6]. In recent years, a wide range of studies have shown the effectiveness of coumarin and its derivatives in regulating enzymes like α-amylase and α-glucosidase [7].

https://dx.doi.org/10.5155/eurjchem.15.3.205-219.2541

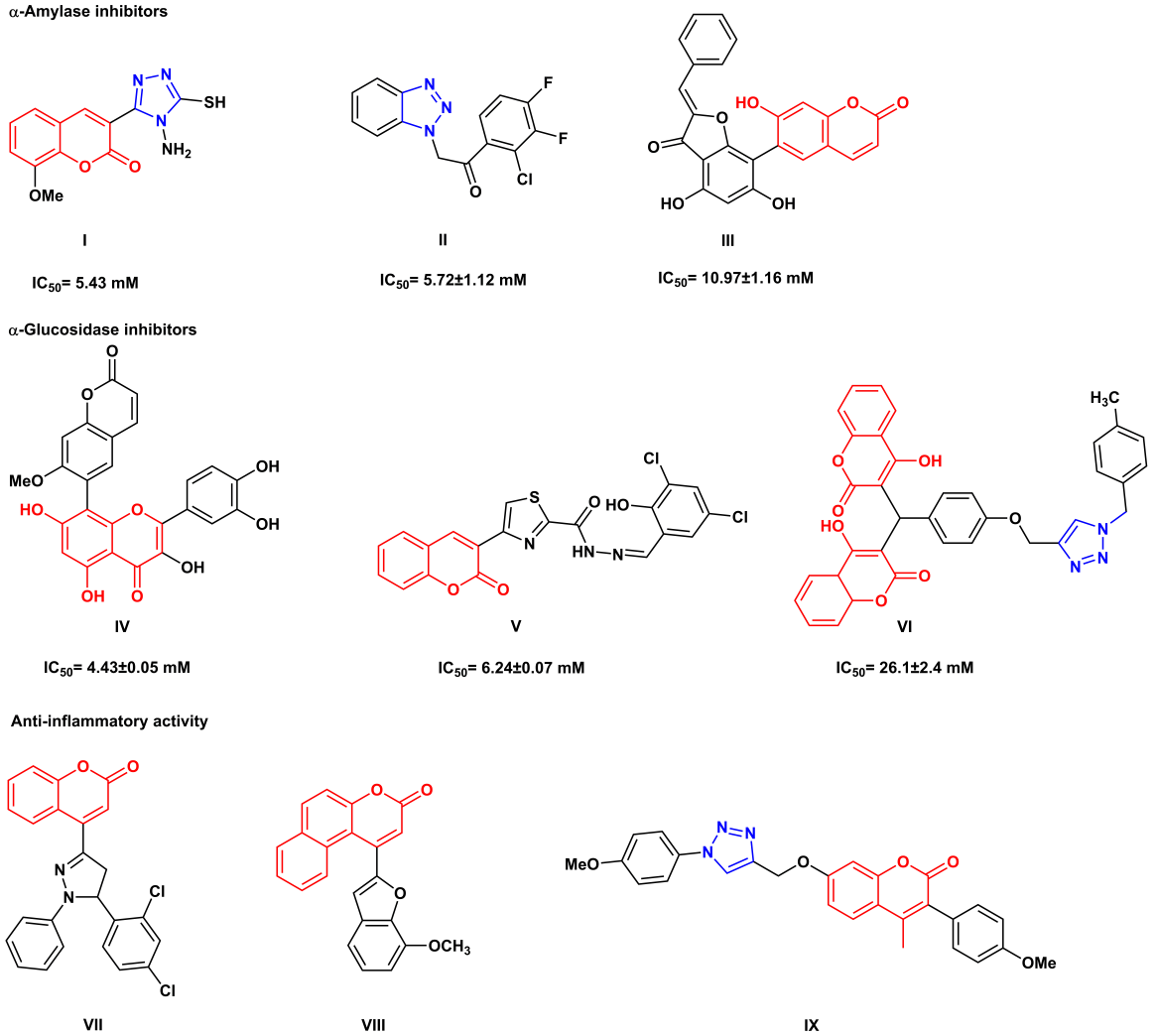

Figure 1. Some of the antidiabetic and anti-inflammatory compounds comprise coumarin and triazole moieties.

Most diabetes treatment focuses on the management of hyperglycemia [8], which is a protocol centered on the reduction of oxidative stress, which is an effective approach for the treatment of diabetes and its related complications. Due to oxidative stress, the generation of reactive oxygen species (ROS) and reactive nitrogen species (RNS) and these free radicals are harmful to living systems [9] resulting inflamemation and other effects. Furthermore, oxidative stress and inflammation are closely related, and several studies indicate that vascular inflammation is caused by arterial diseases. However, the accumulation of ROS at the site of inflammation occurs due to the fact that most cells and leukocytes are produced, leading to a respiratory damage [10]. The dangers associated with the inflammatory process make it difficult for medicinal chemists to develop more effective anti-inflammatory drugs. A significant number of known anti-inflammatory substances, particularly those with clinically demonstrated efficacy, are acidic in character. Non-steroidal anti-inflammatory drugs (NSAIDs) are a prominent family of drugs used to treat inflammation. They operate in affected tissues by blocking the cyclooxygenase (COX) involved in the manufacture of prostaglandins [11-13].

With decades of history and future potential, heterocyclic chemistry has dominated the discipline and is essential for the synthesis of new medications. Coumarins and triazoles have attracted considerable interest among heterocycles due to their widespread natural occurrence and significant biological activity [14]. The glycoside derivatives of naturally occurring coumarins are helpful in medicine [15]. Coumarins are widely used as anticancer [16,17], antidiabetic [18], anti-inflammatory [19,20], antioxidant [21], anticonvulsant [22], antimicrobial [23,24], and antiviral [25] agents.

Coumarin scaffolds are well-known structural motifs that are typically found in plants and a few microorganisms. They were revealed to exhibit a broad range of bioactivities and have emerged as leading candidates for therapeutic applications [26]. Since the development of click chemistry [27], triazoles have been highly yielding, wide in scope, and proven to be potent bioactive pharmacophores [28] that tend to exhibit various biochemical uses, drawing researchers in several disciplines [29]. Despite its unique and broad pharmacological characteristics, extensive efforts have not been made to develop coumarin-triazole-based antidiabetic drugs. However, recent literature findings emphasize the anti-diabetic efficacy of coumarin-moored triazole compounds [14,30], encouraging researchers to synthesize and investigate novel molecular hybrids with improved therapeutic value against α-amylase and α-glucosidase inhibitors. Structures of some of the reported coumarin and triazole moieties possessing good α-amylase inhibitors [31-33], α-glucosidase inhibitors [33-35] and anti-inflammatory agents [36,37] are shown in Figure 1. In an effort to find novel, potential active pharmacophores with promising α-glucosidase inhibitors, α-amylase inhibitors, we have synthesized 12 hybrid scaffolds with good antidiabetic agents

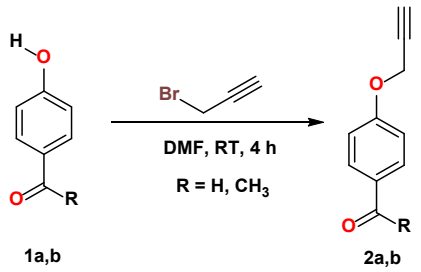

Scheme 1. Synthesis of acetylenic dipolorophile, 2a,b.

and further display better anti-inflammatory activity; they may turn out to be leading candidates for drug development studies.

However, five-membered heterocycles, in particular 1,2,3-triazoles, play a crucial role in medicinal chemistry. 1,2,3-Triazoles were produced using a [3+2] cycloaddition method. Triazoles are widely used as antiviral [38], antimicrobial [39], anti-neuroinflammatory [40], anti-inflammatory [41], anti-plasmodial [42], antidiabetic [43], and anticancer agents [44]. When new or additional pharmacophore quality is added to existing molecules of coumarin derivatives, new structural entities that increase activity with the fewest negative effects may be produced. Various coumarin-triazole-linked derivatives have shown excellent antidiabetic properties [45-49]. The structural similarity between coumarin derivatives and the strong α-glucosidase inhibitor genistein prompted us to investigate the inhibitory activity of coumarin and triazole hybrids as potential candidates in our search for new, easily available, and chemically stable α-glucosidase inhibitors.

2. Experimental

2.1. Material and methods

All starting materials and reagents were analytical grade, obtained from commercial suppliers (Sigma Aldrich, S.D. Fine, Alfa Aesar, and Spectrochem), and used without additional purification. All melting points were determined using a Coslab Scientific melting point device and are unadjusted. Thin layer chromatography (TLC) was used to track reaction rates on precoated Merck silica gel $60F_{254}$ plates using an appropriate solvent system and spots were identified using UV light (λ = 254 nm). IR spectra were collected using potassium bromide (KBr) pellets on a Nicolet 170 SX FTIR spectrometer; the frequencies are reported in cm^{-1}. With a Bruker Avance FT NMR spectrometer with tetramethylsilane as probe, nuclear magnetic resonance (^{1}H NMR, 400 MHz and ^{13}C NMR, 100 MHz) spectra were collected using TMS as an internal standard, using $CDCl_3$ and DMSO-d_6 as a solvent. Shimadzu GCMSQP2010S and ESI/APCI-hybrid quadrupole, time-of-flight, and LC/MS mass spectrometers were used to record mass spectra (Synapt G2 HDMS ACQUITY UPLC). A Heraeus Carlo Erba 1180 CHN analyzer was used to perform elemental studies (C, H and N).

2.2. General synthetic procedure

2.2.1. Synthesis of terminal alkynes, 2a,b

The *p*-hydroxyarylcarbonyl compound (1 equiv.) was disintegrated in DMF and potassium carbonate (1.5 equiv.) was added. Propargyl bromide (1.2 equiv.) was injected dropwise into this solution and the reaction components were stirred at room temperature for 24 h. After the completion of the reaction, which was scrutinized by TLC, it was discharged onto smashed ice, the precipitate was filtered to obtain the product (Scheme 1) [50].

2.2.2. Preparation of 4-(azidomethyl)-2H-chromen-2-ones, 6c-h

4-Bromomethyl coumarin (5c-h) (0.010 mol) was taken in acetone (20 mL) in a round-bottom flask. Sodium azide (0.012 mol) in water (3.00 mL) was added dropwise with stirring, which was continued for 10 h. The reaction mixture was then poured into ice-cold water. The separated solid was filtered and recrystallized from ethanol to obtain the compound 6c-h using the reported method (Scheme 2) [51].

2.2.3. Synthesis of 1,2,3-triazolyl-methyl-2H-chromen-2-ones, 7i-t

The reaction mixture was prepared by taking acetylenic dipolorophile (compounds 2a-b, 0.1 mol) in THF:H_2O mixture (1:1 ratio), followed by the addition of $CuSO_4{\cdot}5H_2O$ (0.015 mol), and sodium ascorbate (0.03 mol). The reaction mixture was stirred at room temperature for half an hour and subsequently 4-(azidomethyl)-2*H*-chromen-2-ones (6c-h) (0.1 mol) were added. The consequential reaction mixture was stirred for one hour, and the completion of the reaction was monitored by TLC. The reaction mixture was then poured into ice cold water. The separated solid was filtered, washed with water and recrystallized with ethyl acetate to obtain the desired product (7i-t) (Scheme 2).

4-([4-([4-Acetylphenoxy]methyl)-1H-1, 2, 3-triazol-1-yl]methyl)-6-methyl-2H-chromen-2-one (7i): Color: White. Yield: 91%. M.p.: 114-116 °C. FT-IR (KBr, ν, cm^{-1}): 1731 (Coumarin, C=O), 1668 (Ketone, C=O). ^{1}H NMR (400 MHz, DMSO-d_6, δ, ppm): 2.37 (s, 3H, CH_3), 2.51 (s, 3H, $C(O)CH_3$), 5.30 (s, 2H, coumarin-C_4-CH_2), 5.78 (s, 1H, coumarin-C_3-H), 5.98 (s, 2H, O-CH_2), 6.77 (d, 1H, *J* = 8.8 Hz, ArH), 7.14 (d, 1H, *J* = 8.8 Hz, ArH), 7.35 (d, 1H, *J* = 8.8 Hz, ArH), 7.49 (d, 1H, *J* = 8.4 Hz, ArH), 7.66 (s, 1H, coumarin-C_5-H), 7.78 (d, 1H, *J* = 8.8 Hz, ArH), 7.92 (d, 1H, *J* = 8.8 Hz, ArH), 8.42 (s, 1H, ArH). ^{13}C NMR (100 MHz, DMSO-d_6, δ, ppm): 20.44, 26.42, 61.27, 85.20, 108.59, 113.69, 114.64, 116.56, 116.62, 117.13, 120.81, 125.95, 130.40, 130.46, 133.46, 133.56, 163.21, 167.55, 178.03, 184.44, 196.4. LC-MS (*m/z*): 390.89 [M+1] 392.89 [M+2]. Elem. anal. calcd. for $C_{22}H_{19}N_3O_4$ (%): C, 67.86; H, 4.92; N, 10.79; Found: C, 67.81; H, 4.94; N, 10.75.

4-([4-([4-Acetylphenoxy]methyl)-1H-1, 2, 3-triazol-1-yl]methyl)-7-methyl-2H-chromen-2-one (7j): Color: Buff. Yield: 93%. M.p.: 124-126 °C. FT-IR (KBr, ν, cm^{-1}): 1730 (Coumarin, C=O), 1672 (Ketone, C=O). ^{1}H NMR (400 MHz, DMSO-d_6, δ, ppm): 2.41 (s, 3H, CH_3), 2.51 (s, 3H, $C(O)CH_3$), 5.29 (s, 2H, coumarin-C_4-CH_2), 5.79 (s, 1H, coumarin-C_3-H), 5.97 (s, 2H, O-CH_2), 7.14 (d, 2H, *J* = 8.8 Hz, ArH), 7.22 (d, 1H, *J* = 8.4 Hz, ArH), 7.28 (s, 1H, coumarin-C_5-H), 7.74 (dd, 1H, *J* = 8.0, 8.8, 14.0 and 14.8 Hz, ArH), 7.92 (d, 2H, *J* = 8.8 Hz, ArH), 8.41 (s, 1H, ArH). ^{13}C NMR (100 MHz, DMSO-d_6, δ, ppm): 21.05, 26.40, 61.26, 112.86, 114.62, 116.85, 124.44, 125.66, 125.85, 130.20, 130.44, 142.82, 150.0, 159.57, 161.73, 194.0, 196.34. LC-MS (*m/z*): 390.98 [M+1], 392.98 [M+2]. Elem. anal. calcd. for $C_{22}H_{19}N_3O_4$ (%): C, 67.86; H, 4.92; N, 10.79; Found:C, 67.90; H, 4.95; N, 10.82.

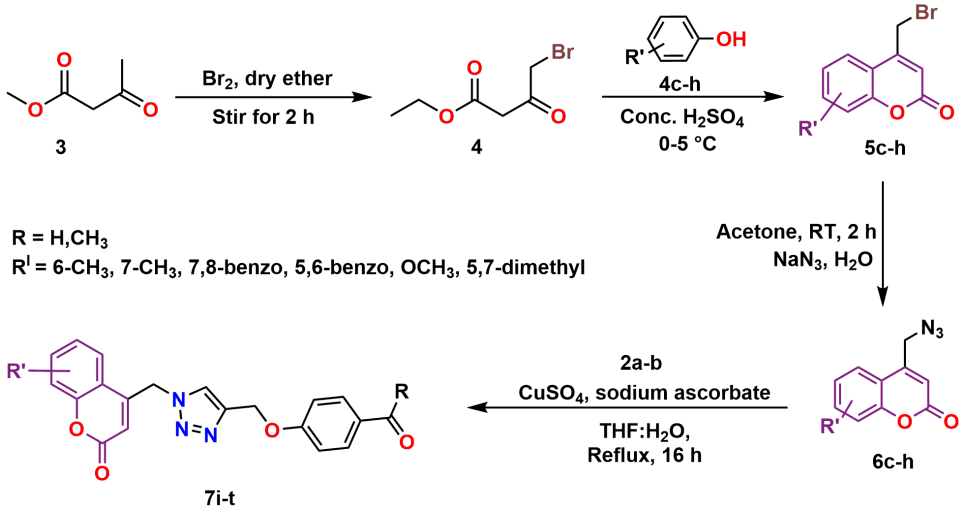

Scheme 2. Schematic depiction of coumarinyl-triazoles, 7i-t.

4-([4-([4-Acetylphenoxy]methyl)-1H-1, 2, 3-triazol-1-yl]methyl)-2H-benzo[h]chromen-2-one (7k): Color: Brown. Yield: 88%. M.p.: 118-120 °C. FT-IR (KBr, ν, cm^{-1}): 1731 (Coumarin, C=O), 1655 (Ketone, C=O). ^{1}H NMR (400 MHz, DMSO-d_6, δ, ppm): 2.48 (s, 3H, C(O)CH$_3$), 5.29 (s, 2H, coumarin-C$_4$-CH$_2$), 5.95 (s, 1H, coumarin-C$_3$-H), 6.09 (s, 2H, O-CH$_2$), 7.13 (d, 2H, *J* = 8.8 Hz, ArH), 7.72-7.75 (m, 2H, ArH), 7.82-7.92 (m, 4H, Ar-H), 8.03-8.06 (m, 1H, ArH), 8.36-8.39 (m, 1H, ArH), 8.43 (s, 1H, ArH). ^{13}C NMR (100 MHz, DMSO-d_6, δ, ppm): 26.4, 49.6, 61.2, 112.8, 113.4, 114.6, 120.3, 121.7, 122.2, 124.3, 125.9, 127.7, 128.0, 129.1, 130.2, 130.4, 150.1, 150.8, 159.3, 161.7, 189.4, 196.3. LC-MS (*m/z*): 426.15 [M+1] 428.15 [M+2]. Elem. anal. calcd. for $C_{25}H_{19}N_3O_4$ (%): C: 70.57; H, 4.55; N, 9.88; Found: C, 70.62; H, 4.45; N, 9.82.

1-([4-([4-Acetylphenoxy]methyl)-1H-1, 2, 3-triazol-1-yl]methyl)-3H-benzo[f]chromen-3-one (7l): Color: Peach. Yield: 92%. M.p.: 130-132 °C. FT-IR (KBr, ν, cm^{-1}): 1735 (Coumarin, C=O), 1668 (Ketone, C=O). ^{1}H NMR (400 MHz, DMSO-d_6, δ, ppm): 2.49 (s, 3H, C(O)CH$_3$), 5.29 (s, 2H, coumarin-C$_4$-CH$_2$), 5.47 (s, 1H, coumarin-C$_3$-H), 6.46 (s, 2H, O-CH$_2$), 7.11 (d, 2H, *J* = 8.4 Hz, ArH), 7.58-7.69 (m, 3H, ArH), 7.87 (d, 2H, *J* = 8.4 Hz, Ar-H), 8.09 (d, 1H, *J* = 8.0 Hz, ArH), 8.25 (d, 1H, *J* = 8.8 Hz, ArH), 8.37 (s, 1H, ArH), 8.43 (d, 1H, *J* = 8.4 Hz, Ar-H). ^{13}C NMR (100 MHz, DMSO-d_6, δ, ppm): 26.5, 53.3, 61.3, 112.5, 113.0, 114.7, 117.5, 125.9, 128.6, 129.8, 130.5, 134.7, 143.0, 152.7, 154.4, 159.1, 161.8, 196.5. LC-MS (*m/z*): 426.15 [M+1], 425.19 [M+]. Elem. anal. calcd. for $C_{25}H_{19}N_3O_4$ (%): C, 70.58; H, 4.50; N, 9.88; Found: C, 70.63; H, 4.49; N, 9.90.

4-([4-([4-Acetylphenoxy]methyl)-1H-1, 2, 3-triazol-1-yl]methyl)-6-methoxy-2H-chromen-2-one (7m): Color: Peach. Yield: 78%. M.p.:150-152 °C. FT-IR (KBr, ν, cm^{-1}): 1712 (Coumarin, C=O), 1694 (Ketone, C=O). ^{1}H NMR (400 MHz, DMSO-d_6, δ, ppm): 2.49 (s, 3H, C(O)CH$_3$), 3.78 (s, 3H, OCH$_3$), 5.28 (s, 2H, coumarin-C$_4$-CH$_2$), 5.86 (s, 1H, coumarin-C$_3$-H), 6.0 (s, 2H, O-CH$_2$), 7.12 (d, 2H, *J* = 8.0 Hz, ArH), 7.23-7.27 (m, 2H, ArH), 7.38 (d, 1H, *J* = 8.8 Hz, ArH), 7.90 (d, 2H, *J* = 8.0 Hz, ArH), 8.41 (s, 1H, ArH). ^{13}C NMR (100 MHz, DMSO-d_6, δ, ppm): 26.4, 49.3, 55.8, 61.2, 107.7, 114.4, 114.6, 117.5, 117.9, 119.6, 125.9, 130.2, 130.4, 147.4, 149.7, 155.6, 159.5, 161.7, 196.3. LC-MS (*m/z*): 406.03 [M+1], 405.03 [M+]. Elem. anal. calcd. for $C_{22}H_{19}N_3O_5$ (%): C, 65.18; H, 4.72; N, 10.37; Found: C, 65.21; H, 4.74; N, 10.35.

4-([4-([4-Acetylphenoxy]methyl)-1H-1, 2, 3-triazol-1-yl]methyl)-5,7-dimethyl-2H-chromen-2-one (7n): Color: Light brown. Yield: 92%. M.p.: 142-144 °C. FT-IR (KBr, ν, cm^{-1}): 1735 (Coumarin, C=O), 1657 (Ketone, C=O). ^{1}H NMR (400 MHz, DMSO-d_6, δ, ppm): 2.43 (s, 3H, CH$_3$), 2.59 (s, 3H, C(O)CH$_3$), 2.76 (s, 3H, CH$_3$), 5.17 (s, 1H, coumarin-C$_3$-H), 5.40 (s, 2H, coumarin-C$_4$-CH$_2$), 6.25 (s, 2H, O-CH$_2$), 7.14 (s, 1H, ArH), 7.21-7.24 (m, 3H, ArH), 8.00 (d, 2H, *J* = 8.8 Hz, ArH), 8.40 (s, 1H, ArH). ^{13}C NMR (100 MHz, DMSO-d_6, δ, ppm): 20.6, 23.3, 26.4, 52.2, 61.3, 114.5, 114.6, 115.6, 126.0, 129.8, 130.2, 130.4, 133.6, 134.1, 136.5, 137.1, 154.6, 159.1, 196.3. LC-MS (*m/z*): 404.12 [M+1], 405.12 [M+2]. Elem. anal. calcd. for $C_{23}H_{21}N_3O_4$ (%): C, 68.47; H, 5.25; N, 10.42; Found: C, 68.50; H, 5.21; N, 10.45.

4-([1-([6-Methyl-2-oxo-2H-chromen-4-yl]methyl)-1H-1, 2, 3-triazol-4-yl]methoxy)benzaldehyde (7o): Color: Cream. Yield: 75%. M.p.: 154-156 °C. FT-IR (KBr, ν, cm^{-1}): 1731 (Coumarin, C=O), 1686 (Aldehyde, C=O). ^{1}H NMR (400 MHz, DMSO-d_6, δ, ppm): 2.25 (s, 3H, CH$_3$), 5.22 (s, 2H, coumarin-C$_4$-CH$_2$), 5.67 (s, 1H, coumarin-C$_3$-H), 5.87 (s, 2H, O-CH$_2$), 7.12 (d, 2H, *J* = 8.8 Hz, ArH), 7.24 (d, 1H, *J* = 8.4 Hz, ArH), 7.37 (d, 1H, *J* = 8.4 Hz, ArH), 7.55 (s, 1H, coumarin-C$_5$-H), 7.75 (d, 2H, *J* = 8.8 Hz, ArH), 8.32 (s, 1H, ArH), 9.76 (s, 1H, CHO). ^{13}C NMR (100 MHz, DMSO-d_6, δ, ppm): 20.4, 49.1, 61.4, 113.7, 115.23, 116.6, 116.8, 124.4, 126.0, 129.9, 131.8, 133.4, 133.9, 142.7, 150.0, 151.2, 159.5, 162.8, 191.3. LC-MS (*m/z*): 376.11 [M+1], 375.11 [M+]. Elem. anal. calcd. for $C_{21}H_{17}N_3O_4$ (%): C, 67.19; H, 4.56; N, 11.19; Found: C, 67.21; H, 4.54; N, 11.15.

4-([1-([7-Methyl-2-oxo-2H-chromen-4-yl]methyl)-1H-1, 2, 3-triazol-4-yl]methoxy)benzaldehyde (7p): Color: Tan. Yield: 91%. M.p.: 178-180 °C. FT-IR (KBr, ν, cm^{-1}): 1721 (Coumarin, C=O), 1671 (Aldehyde, C=O). ^{1}H NMR (400 MHz, DMSO-d_6, δ, ppm): 2.41 (s, 3H, CH$_3$), 5.32 (s, 2H, coumarin-C$_4$-CH$_2$), 5.80 (s, 1H, coumarin-C$_3$-H), 5.97 (s, 2H, O-CH$_2$), 7.21 (m, 3H, *J* = 8.8 Hz, ArH), 7.29 (s, 1H, coumarin-C$_5$-H), 7.73 (d, 1H, *J* = 8.0, 8.8, 14.0 and 14.8 Hz, ArH), 7.85 (d, 2H, *J* = 8.8 Hz, ArH), 8.42 (s, 1H, ArH), 9.87 (s, 1H, CHO). ^{13}C NMR (100 MHz, DMSO-d_6, δ, ppm): 21.1, 49.2, 61.4, 112.9, 114.7, 115.3, 116.9, 124.5, 125.7, 126.0, 129.9, 131.8, 142.7, 143.6, 150.0, 153.2, 156.5, 162.9, 191.4. LC-MS (*m/z*): 376.11 [M+1], 378.11 [M+2]. Elem. anal. calcd. for $C_{21}H_{17}N_3O_4$ (%): C, 67.19; H, 4.56; N, 11.19; Found: C, 67.20; H, 4.55; N, 11.22.

4-([1-([2-Oxo-2H-benzo[h]chromen-4-yl]methyl)-1H-1, 2, 3-triazol-4-yl]methoxy)benzaldehyde (7q): Color: Peach. Yield: 92%. M.p.: 136-138 °C. FT-IR (KBr, ν, cm^{-1}): 1723 (Coumarin, C=O), 1670 (Aldehyde, C=O). ^{1}H NMR (400 MHz, DMSO-d_6, δ, ppm): 5.29 (s, 2H, coumarin-C$_4$-CH$_2$), 5.95 (s, 1H, coumarin-C$_3$-H), 6.09 (s, 2H, O-CH$_2$), 7.13 (d, 2H, *J* = 8.8 Hz, ArH), 7.72-7.75 (m, 2H, ArH), 7.82-7.92 (m, 4H, Ar-H), 8.03-8.06 (m, 1H, ArH), 8.36-8.39 (m, 1H, ArH), 8.43 (s, 1H, ArH), 9.87 (s, 1H, CHO). ^{13}C NMR (100 MHz, DMSO-d_6, δ, ppm): 49.7, 61.4, 112.8, 115.3,

120.3, 121.7, 124.4, 126.1, 127.8, 128.1, 129.2, 130.0, 131.8, 134.5, 149.3, 150.9, 158.9, 158.4, 162.9, 175.7, 183.7, 191.5. LC-MS (*m/z*): 412.16 [M+1], 414.16 [M+2]. Elem. anal. calcd. for $C_{24}H_{17}N_3O_4$ (%): Calcd. C, 70.07; H, 4.17; N, 10.21; Found: C, 70.10; H, 4.15; N, 10.25.

4-([1-([3-Oxo-3H-benzo[f]chromen-1-yl]methyl)-1H-1, 2, 3-triazol-4-yl]methoxy)benzaldehyde (7r): Color: Buff. Yield: 89%. M.p.: 128-130 °C. FT-IR (KBr, ν, cm^{-1}): 1736 (Coumarin, C=O), 1687 (Aldehyde, C=O). ^{1}H NMR (400 MHz, DMSO-d_6, δ, ppm): 5.35 (s, 2H, coumarin-C_4-CH_2), 5.51 (s, 1H, coumarin-C_3-H), 6.49 (s, 2H, O-CH_2), 7.23 (d, 2H, *J* = 8.8 Hz, ArH), 7.62-7.72 (m, 3H, ArH), 7.85-7.88 (m, 2H, Ar-H), 8.10-8.13 (dd, 1H, *J* = 1.0, 1.2, 6.8 and 8.0 Hz, ArH), 8.28 (d, 1H, *J* = 9.2 Hz, ArH), 8.40 (d, 2H, *J* = 8.8 Hz, Ar-H), 9.88 (s, 1H, CHO). ^{13}C NMR (100 MHz, DMSO-d_6, δ, ppm): 53.1, 61.4, 112.4, 112.9, 115.2, 117.4, 125.4, 125.8, 126.1, 128.5, 129.7, 131.7, 134.5, 152.6, 154.3, 158.9, 162.8, 170.3, 191.3. LC-MS (*m/z*): 412.13 [M+1], 413.14 [M+2]. Elem. anal. calcd. for $C_{24}H_{17}N_3O_4$ (%): C, 70.07; H, 4.16; N, 10.21; Found: C, 70.03; H, 4.19; N, 10.20.

4-([1-([6-Methoxy-2-oxo-2H-chromen-4-yl]methyl)-1H-1, 2, 3-triazol-4-yl]methoxy)benzaldehyde (7s): Color: Light pink. Yield: 64%. M.p.: 136-138 °C. FT-IR (KBr, ν, cm^{-1}): 1716 (Coumarin, C=O), 1635 (Aldehyde, C=O). ^{1}H NMR (400 MHz, DMSO-d_6, δ, ppm): 3.72 (s, 3H, OCH_3), 5.25(s, 2H, coumarin-C_4-CH_2), 5.82 (s, 1H, coumarin-C_3-H), 5.93 (s, 2H, O-CH_2), 7.14-7.21 (m, 3H, ArH), 7.33 (d, 1H, *J* = 8.8 Hz, ArH), 7.79 (d, 3H, *J* = 8.4 Hz, ArH), 8.36 (s, 1H, ArH), 9.79 (s, 1H, CHO). ^{13}C NMR (100 MHz, DMSO-d_6, δ, ppm): 49.5, 55.7, 61.3, 106.3, 110.0, 114.2, 115.1, 117.7, 119.4, 125.6, 131.6, 136.6, 148.8, 155.6, 159.3, 164.2, 196.6. LC-MS (*m/z*): 392.02 [M+1], 391.03 [M+]. Elem. anal. calcd. for $C_{21}H_{17}N_3O_5$ (%): C, 64.45; H, 4.38; N, 10.74; Found: C, 64.41; H, 4.34; N, 10.75.

4-([1-([5, 7-Dimethyl-2-oxo-2H-chromen-4-yl]methyl)-1H-1, 2,3-triazol-4-yl]methoxy)benzaldehyde (7t): Color: Buff. Yield: 95%. M.p.: 152-154 °C. FT-IR (KBr, ν, cm^{-1}): 1720 (Coumarin, C=O), 1672 (Aldehyde, C=O). ^{1}H NMR (400 MHz, DMSO-d_6, δ, ppm): 2.42 (s, 3H, CH_3), 2.75 (s, 3H, CH_3), 5.18 (s, 1H, coumarin-C_3-H), 5.42 (s, 2H, coumarin-C_4-CH_2), 6.24 (s, 2H, O-CH_2), 7.13 (s, 1H, ArH), 7.20 (s, 1H, ArH), 7.31 (d, 2H, *J* = 8.8 Hz, ArH), 7.94 (d, 2H, *J* = 8.8 Hz, ArH), 8.41 (s, 1H, ArH), 9.94 (s, 1H, CHO). ^{13}C NMR (100 MHz, DMSO-d_6, δ, ppm): 20.62, 23.3, 61.4, 83.6, 111.5, 115.3, 115.6, 126.1, 129.8, 129.9, 131.8, 136.5, 148.6, 153.0, 154.6, 162.8, 179.4, 191.3. LC-MS (*m/z*): 391.19 [M+2], 390.98 [M+1], 389.98 [M+]. Elem. anal. calcd. for $C_{22}H_{19}N_3O_4$ (%): C, 67.86; H, 4.92; N, 10.79; Found: C, 67.90; H, 4.91; N, 10.75.

2.3. Experimental method for biological evaluation

2.3.1. In vitro α-amylase inhibition assay

In humans, starch is first partially digested by salivary amylase, resulting in the degradation of polymeric substrates into shorter oligomers. Once the oligomers reach the gut, they are further hydrolyzed by pancreatic α-amylase into maltose, maltotriose, and small malto-oligosaccharides. Dietary starch (maltose) is hydrolyzed by the digestive enzyme (α-amylase), which breaks down into glucose prior to absorption. Inhibition of α-amylase can lead to a reduction in postprandial hyperglycemia in diabetic conditions. Thus, *in vitro* antidiabetic activity was examined by α-amylase inhibition potential using the 3,5-dinitro salicylic acid method [52]. Various concentrations of synthesized compounds were preincubated for half an hour with 1% α-amylase. This was considered a test; the negative control or blank was maintained without α-amylase but with distilled water. The positive control was maintained with distilled water and α-amylase. Starch (1%, 1 mL) was added and incubated at 37 °C for 10 min. 1 mL DNSA reagent was added to all test tubes. The test tubes were then incubated in a boiling water bath for 5 min. The OD was taken at 540 nm after cooling the tubes. Acarbose was a standard antidiabetic drug. The experiment was carried out in triplicate. The percentage inhibition of α-amylase activity was determined using the following formula:

$$\text{Inhibition (\%)} = [1 - \frac{B}{A}] \times 100 \quad (1)$$

where A = Absorbance of the control reaction mixture (negative control) and B = Absorbance of the test reaction mixture.

2.3.2. In vitro α-glucosidase inhibition assay

The evaluation of *p*-nitrophenoxide, which is produced from nitrophenol in basic media, is the core of the α-glucosidase inhibition assay [53]. The enzyme glucosidase releases *p*-nitrophenol from *p*-NPG (*p*-nitrophenyl-*α*-D-glucopyranoside). The percentage of inhibition (drop of the light absorption species, *p*-nitrophenoxide) was evaluated in the presence and absence of an inhibitory substance (negative control, 100% of enzyme activity). This percentage of inhibition was considered as the method's response. The experiment was carried out in triplicate. The following equation was used in each case to determine the percentage of inhibition.

$$\text{Inhibition (\%)} = [1 - \frac{B}{A}] \times 100 \quad (2)$$

where A = Control reaction mixture absorbance and B = Test reaction mixture absorbance.

2.3.3. In vitro anti-inflammatory activity by denaturation of bovine serum albumin method

The anti-inflammatory effect of compound 7i-t derivatives was evaluated using the denaturation of bovine serum albumin methodology, as described by Mizushima *et al.* [54] and Sakat *et al.* [55]. The test sample contains the test chemical and a 1% aqueous solution of bovine albumin, and the pH of the reaction mixture was adjusted to 7.4 using appropriate stripping solutions. The test samples were incubated at 37 °C for 20 minutes before being heated to 51 °C for 20 minutes. After being cooled to room temperature, the turbidity of the sample was measured at 660 nm with a UV-visible spectrophotometer. The experiment was carried out in triplicate, with diclofenac sodium serving as the control medication. The percentage inhibition of protein denaturation was determined using the following formula.

$$\text{Inhibition (\%)} = [1 - \frac{B}{A}] \times 100 \quad (3)$$

where A = Absorbance of the control reaction mixture (negative control) and B = Absorbance of the test reaction mixture.

2.4. Molecular docking

The 3D structure of the synthesized compounds in .pdb and .pdbqt formats was prepared using Avogadro software in the optimized geometrical conformations and by applying MMFF94 force field using Open Babel software [56]. The newly synthesized compounds and acarbose were docked against the hypothesized enzyme human pancreatic α-amylase in complex with the carbohydrate inhibitor acarbose (PDB code: 1B2Y) [57]. The protein preparation, including the removal of bound ligands and water molecules that were heteroatoms, the addition of polar hydrogens, the computation of Kollman and Gasteiger charges, and the assignment of other miscellaneous parameters was performed using ADT [58]. Molecular docking was performed using the AutoDock Vina.exe file, with ten modes in four energy ranges in a grid size of 40 Å × 40 Å × 40 at the active site of the enzyme (x: 18.909389, y: 5.790370, z: 47.006148) [59].

Table 1. Optimization of reaction conditions.

Entry	$CuSO_4 \cdot H_2O$ (mol %)	Solvent	Time (h)	Yield (%)
1	10	DMSO	16	18
2	10	Acetonitrile	15	28
3	10	DMF	22	12
4	10	Ethanol	20	45
5	10	Methanol	20	54
6	10	Ethanol:H_2O (1:1)	20	63
7	10	Ethanol:H_2O (2:1)	20	69
8	10	THF:H_2O (1:1)	4	88
9	15	THF:H_2O (1:1)	4	90
10	20	THF:H_2O (1:1)	4	90

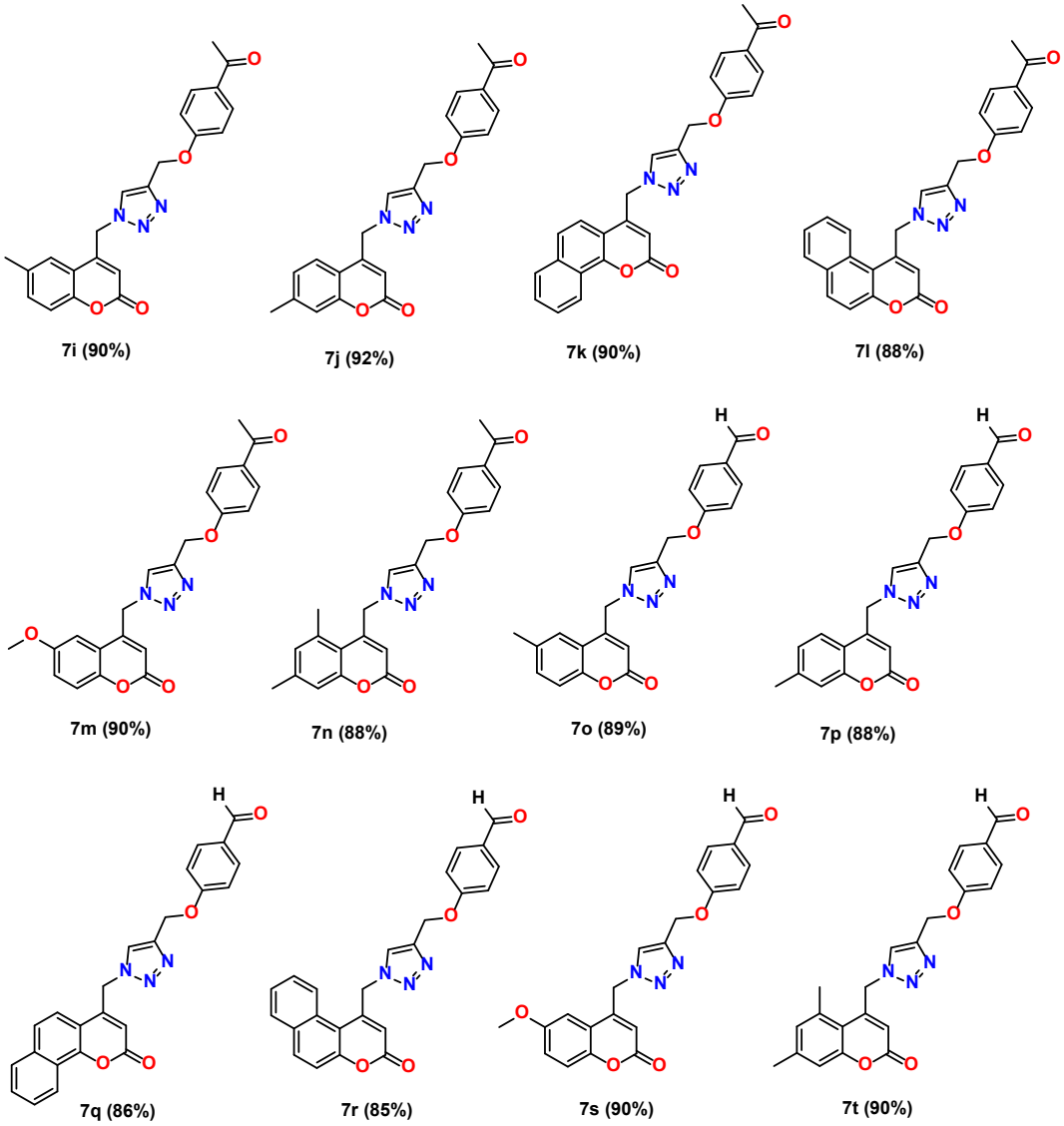

Figure 2. Synthesized coumarinyl-triazoles (7i-t) and their corresponding yields.

3. Results and discussion

3.1. Chemistry

A number of 1,2,3-(triazol-4-yl)-2H-chromen-2-ones (7i-t) were successfully synthesized by a multistep process. In the present study, we intend to report the click-chemistry-tethered regioselective synthesis of 1,2,3-triazolyl-2*H*-chromen-2-one (7i-t) with high yields and purity in short reaction times (Scheme 1). 4-Hydroxy acetophenone/benzoaldehyde was used as the starting material, which upon treatment with propargyl bromide gives terminal alkynes (2a-b). On the other hand, 3-azido methyl coumarins (6c-h) were obtained by the reaction of 3-bromomethyl coumarin with sodium azide in aqueous acetone at room temperature. This was followed by the azide-alkyne cycloaddition of the 3-azido methylcoumarins (6c-h) and acetylenic dipolarophiles (2a-b) (Scheme 2), for which we optimized the reaction conditions using various catalytic amounts of $CuSO_4.5H_2O$ in various solvents, as tabulated in Table 1. The structures of the synthesized compounds 7i-t were verified by ^{1}H NMR, ^{13}C NMR, mass spectroscopic studies, and elemental analysis. The structures of the synthesized coumarinyl-triazoles (7i-t) and their corresponding yields are given in Figure 2.

Table 2. IC_{50} value for inhibition of the α-amylase activity of the synthesized compounds 7i-t *.

Compounds	IC_{50} value (mg/mL)
7i	1.29±0.027
7j	0.92±0.023
7k	0.89±0.017
7l	0.67±0.014
7m	1.10±0.016
7n	0.77±0.023
7o	1.69±0.008
7p	1.16±0.012
7q	0.98±0.013
7r	1.73±0.006
7s	2.31±0.005
7t	0.87±0.009
Acarbose	1.84±0.002

* Values are expressed as mean±SD, n = 3.

Table 3. IC_{50} value of α-glucosidase inhibition of the synthesized compounds 7i-t.

Compounds	IC_{50} value (mg/mL)
7i	1.69±0.023
7j	0.99±0.026
7k	0.96±0.013
7l	0.72±0.012
7m	1.38±0.017
7n	0.81±0.021
7o	1.97±0.009
7p	1.30±0.014
7q	1.20±0.015
7r	2.28±0.007
7s	3.27±0.004
7t	0.99±0.006
Acarbose	1.41±0.005

* Values are expressed as mean±SD, n = 3.

Solvent optimization was performed using various protic and aprotic solvents. Some commonly used solvents such as DMSO, ACN, DMF, ethanol, methanol, and THF, and a combination of these solvents are also used under reflux conditions to get products. Initially, DMSO, ACN, and DMF were used to obtain the products, but the yields were initially very low with the use of a 10 mol% catalyst, that is, (Table 1, Entries 1-3). The reaction was further extended and performed in protic solvents such as ethanol, methanol, and THF, and a mixture of water solvents. In the case of ethanol and methanol (Table 1, Entrys 4,5) and with water mixtures (Table 1, Entrys 6,7) here we noticed the formation of the product. But the reaction was completed after prolonged time and the isolated yields are 45-70%. Later, we increased the catalyst concentration to 15 mol%; the product resulted in a 90% yield (Table 1, Entry 8). When the catalyst concentration increased by 20 mol%, isolated yield changes were not found (Table 1, Entry 10). Some reactions were performed at ambient temperature; the result was found to be poor. We observed that the percentage yield of the products (7i-t) was higher in the alcohol and water mixture compared to the solvent alone. Then we decided to perform the reaction in THF with a water mixture; surprisingly, the product formation and completion of the reaction occurred in a short time, and the isolated yield is more than 85%.

3.2. Biological studies

3.2.1. Inhibition of α-amylase activity

To investigate the pharmacological significance of these synthesized molecules, all hybrids were evaluated for their antidiabetic ability [60]. Therapeutic investigation to treat diabetes is to reduce postprandial hyperglycemia. This can be done by suppressing the absorption of glucose via inhibition of the sugar hydrolysing enzymes, particularly α-amylase [46] and α-glucosidase [53] in the digestive system [61].

Table 2 provides IC_{50} data of the findings of the study on α-amylase inhibition. Interestingly, the synthesized compound 7i-t exhibited a large impact on starch utilization and IC_{50} results of the compounds with the standard drug acarbose. Compounds 7l and 7n demonstrated excellent inhibition with values of 0.67±0.014 and 0.77±0.023 mg/mL, respectively. While compounds 7o, 7r, and 7s showed a moderate amount of α-amylase inhibition with IC50 values of 1.69±0.008, 1.73±0.006, and 2.31±0.005 mg/mL, respectively. Compound 7l exhibited the highest inhibition of the enzyme among all derivatives. From the study, we conclude that most synthesized compounds have more effectively shown inhibition of α-amylase compared to the standard drug.

3.2.2. In vitro α-glucosidase inhibition activity

All compounds were screened for α-glucosidase inhibition profile with the help of *p*-NPG, the percentage inhibition was calculated and the IC_{50} values were determined [62]. All compounds exhibit excellent inhibition profiles except compounds 7r and 7s compared to the standard drug acarbose. Table 3 reveals that compound 7l showed significant glucosidase inhibition potency with the IC_{50} value of 0.72±0.012 mg/mL among all synthesized 7i-t compounds.

3.2.3. In vitro anti-inflammatory activity

Synthesized **7i-t** derivatives were evaluated for their anti-inflammatory efficacy using the protein denaturation inhibition technique with diclofenac sodium as the reference medication. The percentage inhibition of the synthesized compounds was measured using different concentrations ranging from 20 to 100 mg/mL. Table 4 lists the results of the IC_{50} values. Among the synthesized compounds, 7o, 7r, 7p, and 7q possessed excellent anti-inflammatory efficiencies with IC_{50} values of 0.54±0.003, 0.55±0.008, 0.57±0.85, and 0.60±0.011 mg/mL, respectively. Compounds 7i, 7j, 7k, 7l, 7m, 7n, 7s, and 7t exhibited moderate inhibition profiles with IC_{50} values of 0.70±0.021, 0.99±0.023, 1.11±0.017, 0.86±0.011, 0.77±0.013, 0.73±0.024, 1.41±0.006, and 1.72±0.007 mg/mL, respectively.

Table 4. IC_{50} anti-inflammatory activity of the synthesized compounds 7i-t *.

Compounds	IC_{50} value (mg/mL)
7i	0.70±0.021
7j	0.99±0.023
7k	1.11±0.017
7l	0.86±0.011
7m	0.77±0.013
7n	0.73±0.024
7o	0.54±0.003
7p	0.57±0.015
7q	0.60±0.011
7r	0.55±0.008
7s	1.41±0.006
7t	1.72±0.007
Diclofenac	0.67±0.004

* Values are expressed as mean±SD, n = 3.

3.3. Computational studies

3.3.1. Molecular docking studies

The use of molecular docking is an emerging method in structure-based drug discovery to evaluate the binding conformation of tiny ligands to the appropriate protein target binding site. They proposed a possible mechanism of α-amylase activity and detailed intermolecular interactions between the synthesized compounds and the postulated protein. The docking studies produced a possible picture of drug-receptor interactions, with nine potential interactions for each compound with the protein. The best possible interaction with the lowest binding energy is visualized using the BIOVIA Discovery Studio 2021 visualizer (Figures 3 and 4). Details such as the binding energy, type of interactions, bond distance, and type of bonding of the possible interactions are listed in Table 5. It is clearly observed in Figures 3 and 4, the compounds 7k and 7q bearing benzo substitution on the coumarin ring showed the highest interaction with amylase protein than acarbose. The compound 7k forms three conventional hydrogen bonds (GLN63: H–O_1; TYR151: OH–O_4), one C-H bond, one π-anion electrostatic interaction, nine hydrophobic interactions (six π-πstacked, one π-πT shaped, two π-alkyl) with a binding energy of -10.6 kcal/mol. Compound 7q forms two conventional hydrogen bonds (GLN63: H–O_1; TYR151: OH–O_4), one C-H bond, one π-anion electrostatic interaction, eleven hydrophobic interactions (six π-πstacked, two π-π T shaped, three π-alkyl) with a binding energy of -10.3 kcal/mol. However, the standard drug acarbose forms 18 conventional hydrogen bonds, three π-donar hydrogen bond interactions, one hydrophobic π-alkyl interaction with a binding energy of -9.9 kcal/mol. This implies that the molecules docked, despite their difference in biological activity, have shown good results with respect to the standard drug. In addition, compounds 7i, 7j, 7l and 7r also showed good interaction comparable to the standard drug acarbose. Compound 7i forms two conventional hydrogen bonds (GLN63: H–O_1; TYR151: OH–O_4), one π-anion electrostatic interaction, ten hydrophobic interactions (one π-sigma, four π-π stacked, one π-π T shaped, four with π-alkyl) with a binding energy of -9.8 kcal/mol similarly, compound 7j forms two conventional hydrogen bonds (GLN63: H–O_1; TYR151: OH–O_4), one π-anion electrostatic interaction, eleven hydrophobic interactions (five π-π stacked, one π-π T shaped, five with π-alkyl) with a binding energy of -9.8 kcal/mol, while compound 7l forms two conventional hydrogen bonds (GLN63: H–O_1; TYR151: OH–O_4), two C-H bonds, one π-anion electrostatic interaction, nine hydrophobic interactions (four π-π stacked, one π-π T shaped, two π-alkyl and one π-donar hydrogen bond) with a binding energy of -9.9 kcal/mol. Compound 7r forms two conventional hydrogen bonds (GLN63: H–O_1; TYR151: OH–O_4), one π-donar interaction, one π-sigma interaction, eleven hydrophobic interactions (two π-π stacked, one π-π T shaped, five with π-alkyl) with a binding energy of -9.8 kcal/mol whereas compounds 7m, 7n, 7o, 7p, 7s, and 7t showed less interaction compared to standard drugs. Compound 7m forms two conventional hydrogen bonds (GLN63: H–O_1; TYR151: OH–O_4), one C-H bonds, one π-anion electrostatic interaction, eleven hydrophobic interactions (four π-π stacked, two π-π T shaped, four with π-alkyl) with binding energy of -9.5 kcal/mol. Although compound 7n forms two conventional hydrogen bonds (GLN63: H–O_1; TYR151: OH–O_4), one C-H bond, two π-anion electrostatic interactions, one π-donor hydrogen bond interaction, eleven hydrophobic interactions (three π-sigma bonds, two π-π stacked, two π-π T shaped, four with π-alkyl) with binding energy of -9.5 kcal/mol. Compound 7o forms one conventional hydrogen bond (GLN63: H–O_1; TYR151: OH–O_4), one C-H bonds, one π-anion electrostatic interaction, nine hydrophobic interactions (three π-sigma bonds, four π-π stacked, one π-π T shaped, four π-alkyl) with binding energy of -9.4 kcal/mol. Similarly, compound 7p forms two conventional hydrogen bonds (GLN63: H–O_1; TYR151: OH–O_4), one C-H bonds, one π-anion electrostatic interaction, ten hydrophobic interactions (three π-sigma bonds, four π-π stacked, two π-π T shaped, four π-alkyl) with binding energy of -9.4 kcal/mol. Compound 7s forms two conventional hydrogen bonds (GLN63: H–O_1; TYR151: OH–O_4), one C-H bond, one π-anion electrostatic interaction, eleven hydrophobic interactions (five π-π stacked, two π-π T shaped, four π-alkyl) with a binding energy of -9.1 kcal/mol. Compound 7t forms two conventional hydrogen bonds (GLN63: H–O_1; TYR151: OH–O_4), one π-anion interaction, one π-sigma interaction, and four hydrophobic interactions (three π-π stacked, one with π-alkyl) with a binding energy of -9.0 kcal/mol. These studies might be initiated to promote the development of the most potent drug molecule against targeting α-amylase and α-glucosidase. As depicted in Figure 4, all synthesized compounds were properly placed in the active site pocket of the α-amylase protein, showing more than ten strong contacts with excellent binding energy compared to the drug acarbose.

4. Structure activity relationship studies

Observing the antihyperglycemic data (Tables 2 and 3), it can be seen that the keto derivatives (7i-n) are more potent molecules than the aldehydic derivatives (7o-t) molecular hybrids. However, it is clearly proven that substitution in the coumarin ring has a substantial effect on the α-amylase and α-glucosidase activity, 6-methyl (7i,o), methoxy substitution (7m, s) has decreased the potency, while substitution of 7-methyl (7j, p), dimethyl (7n, t) and benzo (7k, l, q, r) substitution have proved to be necessary for good.

When comparing antidiabetic and anti-inflammatory activity with respect to aldehydic 7o-t and keto substitution, it was clear that keto 7i-n has a strong antidiabetic tendency whereas aldehydic derivatives have shown a strong anti-inflammatory effect (Table 4). Furthermore, the substitution of 6-methyl (7o,p), (7q,r) benzo in the coumarin ring has resulted

Table 5. Details of the best possible interaction of compound 7i-t, newly synthesized compounds, and acarbose (Ac) with the enzyme human pancreatic α-amylase (1B2Y).

Inhibitor	Binding energy (kcal/ mol)	Interactions	Distance (Å)	Bonding	Types of bonding
7i	-9.8	(GLN63) H – O_1	2.28632	Hydrogen	Conventional
		(TYR151) OH – O_4	3.36470	Hydrogen	Conventional
		(ASP300) O – π (N_1-C_{12})	3.39924	Pi-Anion	Electrostatic
		(LEU162) C – π (C_{14}-C_{19})	3.93218	Pi-Sigma	Hydrophobic
		π (TRP59) – π (C_1-C_6)	3.87733	Pi-Pi Stacked	Hydrophobic
		π (TRP59) – π (C_4-O_1)	4.93615	Pi-Pi Stacked	Hydrophobic
		π (TRP59) – π (C_1-C_6)	3.81425	Pi-Pi Stacked	Hydrophobic
		π (TRP59) – π (C_4-O_1)	5.03580	Pi-Pi Stacked	Hydrophobic
		π (N_1-C_{12}) – π (TYR62)	4.91665	Pi-Pi T-shaped	Hydrophobic
		π (TRP59) – C_{22}	4.01571	Pi-Alkyl	Hydrophobic
		π (TRP59) – C_{22}	4.47553	Pi-Alkyl	Hydrophobic
		π (HIS305) – C_{22}	4.95912	Pi-Alkyl	Hydrophobic
		π (C_{14}-C_{19}) – (ALA198)	5.14104	Pi-Alkyl	Hydrophobic
7j	-9.8	(GLN63) H – O_1	2.28129	Hydrogen	Conventional
		(TYR151) H – O_4	2.28352	Hydrogen	Conventional
		(ASP300) O – π (N_1-C_{12})	3.44223	Electrostatic	Pi-Anion
		π (TRP59) – C_{22}	3.89332	Hydrophobic	Pi-Pi Stacked
		π (TRP59) – π (C_1-C_6)	4.86930	Hydrophobic	Pi-Pi Stacked
		π (TRP59) – π (C_1-C_6)	3.79364	Hydrophobic	Pi-Pi Stacked
		π (TRP59) – π (C_4-O_1)	4.94750	Hydrophobic	Pi-Pi Stacked
		π (N_1-C_{12}) – π (TRP58)	5.10755	Hydrophobic	Pi-Pi Stacked
		π (N_1-C_{12}) – π (TYR62)	4.92972	Hydrophobic	Pi-Pi T-shaped
		π (TRP59) – C_{10}	4.07646	Hydrophobic	Pi-Alkyl
		π (TRP59) – C_{22}	4.48723	Hydrophobic	Pi-Alkyl
		π (HIS305) – C_{22}	5.06349	Hydrophobic	Pi-Alkyl
		π (C_{14}-C_{19}) – (LEU162)	4.56941	Hydrophobic	Pi-Alkyl
		π (C_{14}-C_{19}) – (ALA198)	5.11186	Hydrophobic	Pi-Alkyl
7k	-10.6	(GLN63) H – O_1	2.40121	Hydrogen	Conventional
		(LYS200) H – O_4	3.00452	Hydrogen	Conventional
		(LYS200) H – O_3	2.85598	Hydrogen	Conventional
		C_{13} – H (GLU233)	3.55294	Carbon Hydrogen	C H Bond
		(ASP300) – π (N_1-C_{12})	3.50353	Electrostatic	Pi-Anion
		(TRP59) – π (C_2-C_{25})	3.86331	Hydrophobic	Pi-Pi Stacked
		(TRP59) – π (N_1-C_{12})	4.54653	Hydrophobic	Pi-Pi Stacked
		(TRP59) – π (C_2-C_{25})	5.06708	Hydrophobic	Pi-Pi Stacked
		(TRP59) – π (C_2-C_{25})	4.11828	Hydrophobic	Pi-Pi Stacked
		(TRP59) – π (C_4-O_1)	3.67030	Hydrophobic	Pi-Pi Stacked
		(TRP59) – π (N_1-C_{12})	5.27908	Hydrophobic	Pi-Pi Stacked
		(HIS201) – π (C_{14}-C_{19})	4.91165	Hydrophobic	Pi-Pi T-shaped
		π (C_{14}-C_{19}) – (LEU162)	4.80230	Hydrophobic	Pi-Alkyl
		π (C_{14}-C_{19}) – (ALA198)	5.05869	Hydrophobic	Pi-Alkyl
7l	-9.9	(LYS200) H – O_4	2.65835	Hydrogen	Conventional
		(ILE235) H – O_4	2.49055	Hydrogen	Conventional
		(GLY306) H – N_3	2.59004	Carbon Hydrogen	C H Bond
		C_{10} – H(ASP300)	3.60089	Carbon Hydrogen	C H Bond
		(HIS305) H – π (N_1-C_{12})	3.18329	Hydrogen	Pi-Donor Hydrogen Bond
		π (TRP59) – π (C_1-C_{25})	5.60961	Hydrophobic	Pi-Pi Stacked
		π (TRP59) – π (C_1-C_6)	4.04262	Hydrophobic	Pi-Pi Stacked
		π (TRP59) – π (C_1-C_{25})	5.83991	Hydrophobic	Pi-Pi Stacked
		π (TRP59) – π (C_1-C_6)	4.28353	Hydrophobic	Pi-Pi Stacked
		π (HIS201) – π (C_{14}-C_{19})	4.79521	Hydrophobic	Pi-Pi T-shaped
		π (C_1-C_6) – (LEU165)	5.30003	Hydrophobic	Pi-Alkyl
		π (C_{14}-C_{19}) – (LEU162)	4.80556	Hydrophobic	Pi-Alkyl
		π (C_{14}-C_{19}) – (ILE235)	5.39262	Hydrophobic	Pi-Alkyl
7m	-9.5	(GLN63) H – O_1	2.35929	Hydrogen	Conventional
		(TYR151) H – O_4	2.27798	Hydrogen	Conventional
		(HIS305) H – O_3	2.68643	Carbon Hydrogen	C H Bond
		(ASP300) O – π (N_1-C_{12})	3.39505	Electrostatic	Pi-Anion
		π (TRP59) – π (C_4-O_1)	3.86449	Hydrophobic	Pi-Pi Stacked
		π (TRP59) – π (C_1-C_6)	4.96672	Hydrophobic	Pi-Pi Stacked
		π (TRP59) – π (N_1-C_{12})	3.90701	Hydrophobic	Pi-Pi Stacked
		π (TRP59) – π (C_4-O_1)	5.12486	Hydrophobic	Pi-Pi Stacked
		π (HIS201) – π (C_{14}-C_{19})	5.08556	Hydrophobic	Pi-Pi T-shaped
		π (N_1-C_{12}) – π (TYR62)	4.86631	Hydrophobic	Pi-Pi T-shaped
		π (TRP59) – C_{22}	4.22427	Hydrophobic	Pi-Alkyl
		π (TRP59) – C_{22}	4.46808	Hydrophobic	Pi-Alkyl
		π (C_{14}-C_{19}) – (LEU162)	4.61837	Hydrophobic	Pi-Alkyl
		π (C_{14}-C_{19}) – (ALA198)	5.04773	Hydrophobic	Pi-Alkyl
7n	-9.5	(GLN63) – O_4	2.39519	Hydrogen	Conventional
		(THR163) – O_2	2.36131	Hydrogen	Conventional
		C_{12} – (ASP300)	3.75949	Carbon Hydrogen	C H Bond
		(ASP197) O – π (N_1-C_{12})	3.70862	Electrostatic	Pi-Anion
		(GLU233) O – π (N_1-C_{12})	4.33018	Electrostatic	Pi-Anion
		(TYR151) H – π (C_1-C_6)	3.02542	Hydrogen	Pi-Donor Hydrogen Bond
		(LEU162) H – π (C_4-O_1)	2.39213	Hydrophobic	Pi-Sigma
		C_{21} – π (TRP59)	3.90543	Hydrophobic	Pi-Sigma
		C_{13} – π (TRP59)	3.70491	Hydrophobic	Pi-Sigma
		π (TRP59) – π (C_{14}-C_{19})	5.08035	Hydrophobic	Pi-Pi Stacked
		π (TYR151) – π (C_1-C_6)	5.54510	Hydrophobic	Pi-Pi Stacked

Table 5. (Continued).

Inhibitor	Binding energy (kcal/ mol)	Interactions	Distance (Å)	Bonding	Types of bonding
7n	-9.5	π (HIS201) – π (C_1-C_6)	4.99780	Hydrophobic	Pi-Pi T-shaped
		π (N_1-C_{12}) – π (TYR62)	5.60432	Hydrophobic	Pi-Pi T-shaped
		π (TYR151) – C_{23}	4.01717	Hydrophobic	Pi-Alkyl
		π (N_1-C_{12})– (ALA198)	4.85305	Hydrophobic	Pi-Alkyl
		π (C_4-O_1) – (LEU162)	5.47430	Hydrophobic	Pi-Alkyl
		π (C_4-O_1) – (ILE235)	5.02353	Hydrophobic	Pi-Alkyl
7o	-9.4	(GLN63) H – O_1	2.31575	Hydrogen	Conventional
		(ASP300) O – π (N_1-C_{12})	3.38018	Electrostatic	Pi-Anion
		(TRP59) – π (C_4-O_1)	3.90422	Hydrophobic	Pi-Pi Stacked
		(TRP59) – π (C_1-C_6)	5.01531	Hydrophobic	Pi-Pi Stacked
		(TRP59) – π (C_4-O_1)	3.85749	Hydrophobic	Pi-Pi Stacked
		(TRP59 – π (C_1-C_6)	5.13778	Hydrophobic	Pi-Pi Stacked
		π (N_1-C_{12}) – (TYR62)	4.95463	Hydrophobic	Pi-Pi T-shaped
		π (TRP59) – C_{21}	3.96179	Hydrophobic	Pi-Alkyl
		π (TRP59) – C_{10}	4.42755	Hydrophobic	Pi-Alkyl
		π (HIS305) – C_{21}	4.94644	Hydrophobic	Pi-Alkyl
		π (C_{14}-C_{19}) – C (ILE235)	5.16866	Hydrophobic	Pi-Alkyl
7p	-9.4	(GLN63) H – O_1	2.33823	Hydrogen	Conventional
		(LYS200) H – O_4	2.75495	Hydrogen	Conventional
		C_{13} – (ASP197)	3.79620	Carbon Hydrogen	C H Bond
		(ASP300) O – π (N_1-C_{12})	3.44066	Electrostatic	Pi-Anion
		(TRP59) – π (C_4-O_1)	3.89214	Hydrophobic	Pi-Pi Stacked
		(TRP59) – π (C_1-C_6)	4.92557	Hydrophobic	Pi-Pi Stacked
		(TRP59) – π (C_4-O_1)	3.91536	Hydrophobic	Pi-Pi Stacked
		(TRP59) – π (C_4-O_1)	5.07707	Hydrophobic	Pi-Pi Stacked
		(HIS201) – π (C_{14}-C_{19})	4.99984	Hydrophobic	Pi-Pi T-shaped
		π (C_{14}-C_{19}) – (TYR62)	4.86139	Hydrophobic	Pi-Pi T-shaped
		(TRP59) – C_{21}	4.81070	Hydrophobic	Pi-Alkyl
		(TRP59) – C_2	3.93727	Hydrophobic	Pi-Alkyl
		π (C_{14}-C_{19}) – (LEU162)	4.64906	Hydrophobic	Pi-Alkyl
		π (C_{14}-C_{19}) – (ALA198)	5.00874	Hydrophobic	Pi-Alkyl
7q	-10.3	(GLN63) H – O_1	2.41250	Hydrogen	Conventional
		(LYS200) H – O_4	2.84496	Hydrogen	Conventional
		C_{13} – (GLU233)	3.49525	Carbon Hydrogen	C H Bond
		π (ASP300) – π (N_1-C_{12})	3.46588	Electrostatic	Pi-Anion
		π (TRP59) – π (C_1-C_6)	3.88158	Hydrophobic	Pi-Pi Stacked
		π (TRP59) – π (C_4-O_1)	4.55721	Hydrophobic	Pi-Pi Stacked
		π (TRP59) – π (C_1-C_{25})	5.06047	Hydrophobic	Pi-Pi Stacked
		π (TRP59) – π (C_4-O_1)	4.13392	Hydrophobic	Pi-Pi Stacked
		π (TRP59) – π (C_1-C_6)	3.67432	Hydrophobic	Pi-Pi Stacked
		π (TRP59) – π (C_1-C_{25})	5.28316	Hydrophobic	Pi-Pi Stacked
		π (HIS201) – π (C_{14}-C_{19})	4.83253	Hydrophobic	Pi-Pi T-shaped
		π (N_1-C_{12}) – (TYR62)	4.80416	Hydrophobic	Pi-Pi T-shaped
		π (C_{14}-C_{19}) – (LEU162)	4.99288	Hydrophobic	Pi-Alkyl
		π (C_{14}-C_{19}) – (ALA198)	5.09360	Hydrophobic	Pi-Alkyl
		π (C_{14}-C_{19}) – (ILE235)	5.25722	Hydrophobic	Pi-Alkyl
7r	-9.8	(THR163) H – C_{12}	2.80093	Carbon Hydrogen	C H Bond
		C_{20} – (HIS299)	3.38207	Carbon Hydrogen	C H Bond
		(TYR151) – π (C_1-C_{25})	2.76766	Hydrogen	Pi-Donor
		(ILE235) – π (C_1-C_6)	2.61306	Hydrophobic	Pi-Sigma
		(TYR62) – π (C_{14}-C_{19})	4.23699	Hydrophobic	Pi-Pi Stacked
		(TYR151) – π (C_1-C_{25})	4.68755	Hydrophobic	Pi-Pi Stacked
		(HIS201) – π (C_1-C_6)	4.63528	Hydrophobic	Pi-Pi T-shaped
		π (C_1-C_6) – (LYS200)	5.37394	Hydrophobic	Pi-Alkyl
		π (C_1-C_6) – (ILE235)	5.43290	Hydrophobic	Pi-Alkyl
		π (C_4-O_1) – (LEU162)	4.71975	Hydrophobic	Pi-Alkyl
		π (C_4-O_1) – (ALA198)	4.87821	Hydrophobic	Pi-Alkyl
		π (C_{14}-C_{19}) – (LEU162)	4.83850	Hydrophobic	Pi-Alkyl
7s	-9.1	(GLN63) H – O_1	2.34111	Hydrogen	Conventional
		(TYR151) H – O_4	2.45881	Hydrogen	Conventional
		(HIS305) H – C_{21}	2.76795	Hydrogen	C H Bond
		π (ASP300) – π (N_1-C_{12})	3.40185	Electrostatic	Pi-Anion
		π (TRP59) – π (C_1-C_6)	3.85899	Hydrophobic	Pi-Pi Stacked
		π (TRP59) – π (C_4-O_1)	4.95810	Hydrophobic	Pi-Pi Stacked
		π (TRP59) – π (C_1-C_6)	3.86331	Hydrophobic	Pi-Pi Stacked
		π (TRP59) – π (C_4-O_1)	5.09627	Hydrophobic	Pi-Pi Stacked
		π (N_1-C_{12}) – π (TRP58)	5.29984	Hydrophobic	Pi-Pi Stacked
		π (HIS201) – π (C_{14}-C_{19})	4.99122	Hydrophobic	Pi-Pi T-shaped
		π (N_1-C_{12}) – π (TYR62)	4.97009	Hydrophobic	Pi-Pi T-shaped
		π (TRP59) – C_{21}	4.44170	Hydrophobic	Pi-Alkyl
		π (TRP59) – C_{21}	4.59693	Hydrophobic	Pi-Alkyl
		π (C_{14}-C_{19}) – (LEU162)	4.84764	Hydrophobic	Pi-Alkyl
		π (C_{14}-C_{19}) – (ALA198	4.95460	Hydrophobic	Pi-Alkyl
7t	-9.0	(GLN63) H – O_4	2.19103	Hydrogen	Conventional
		(THR163) H – O_2	2.69678	Hydrogen	Conventional
		(GLU233) O – π (N_1-C_{12})	4.01980	Electrostatic	Pi-Anion
		C_{22} – π (TYR151)	3.78505	Hydrophobic	Pi-Sigma
		π (TYR62) – π (C_{14}-C_{19})	4.87241	Hydrophobic	Pi-Pi Stacked
		π (TYR151 – π (C_1-C_6)	4.18966	Hydrophobic	Pi-Pi Stacked
		π (TYR151 – π (C_4-O_1)	5.63588	Hydrophobic	Pi-Pi Stacked
		π (C_4-O_1) – (LEU162)	5.20264	Hydrophobic	Pi-Alkyl

Table 5. (Continued).

Inhibitor	Binding energy (kcal/ mol)	Interactions	Distance (Å)	Bonding	Types of bonding
Acarbose	-9.9	(GLN63) – O_6	2.92098	Hydrogen	Conventional
		(GLN63) – O_5	2.96298	Hydrogen	Conventional
		(ARG195) – O_2	2.77415	Hydrogen	Conventional
		(LYS200) – O_2	2.45335	Hydrogen	Conventional
		(LYS200) – O_3	2.87745	Hydrogen	Conventional
		(HIS305) – O_2	2.95637	Hydrogen	Conventional
		O_2 – (GLU240)	3.19011	Hydrogen	Conventional
		O_2 – (HIS20)	2.63086	Hydrogen	Conventional
		O_3 – (GLU233)	2.75598	Hydrogen	Conventional
		N_4 – (GLU233)	2.92776	Hydrogen	Conventional
		O_2 – (GLU233)	3.32628	Hydrogen	Conventional
		O_2 – (ASP300)	2.66732	Hydrogen	Conventional
		O_3 – (HIS299)	2.70233	Hydrogen	Conventional
		O_6 – (ASP197)	2.83914	Hydrogen	Conventional
		O_6 – (TRP59)	2.51729	Hydrogen	Conventional
		O_4 – (THR163)	3.10358	Hydrogen	Conventional
		O_3 – (TYR62)	3.50463	Hydrogen	Pi-Donor
		O_2 – (TRP59)	3.84471	Hydrogen	Pi-Donor
		O_2 – (TRP59)	3.67806	Hydrogen	Pi-Donor
		C_6 – (LEU165)	4.31121	Hydrophobic	Alkyl

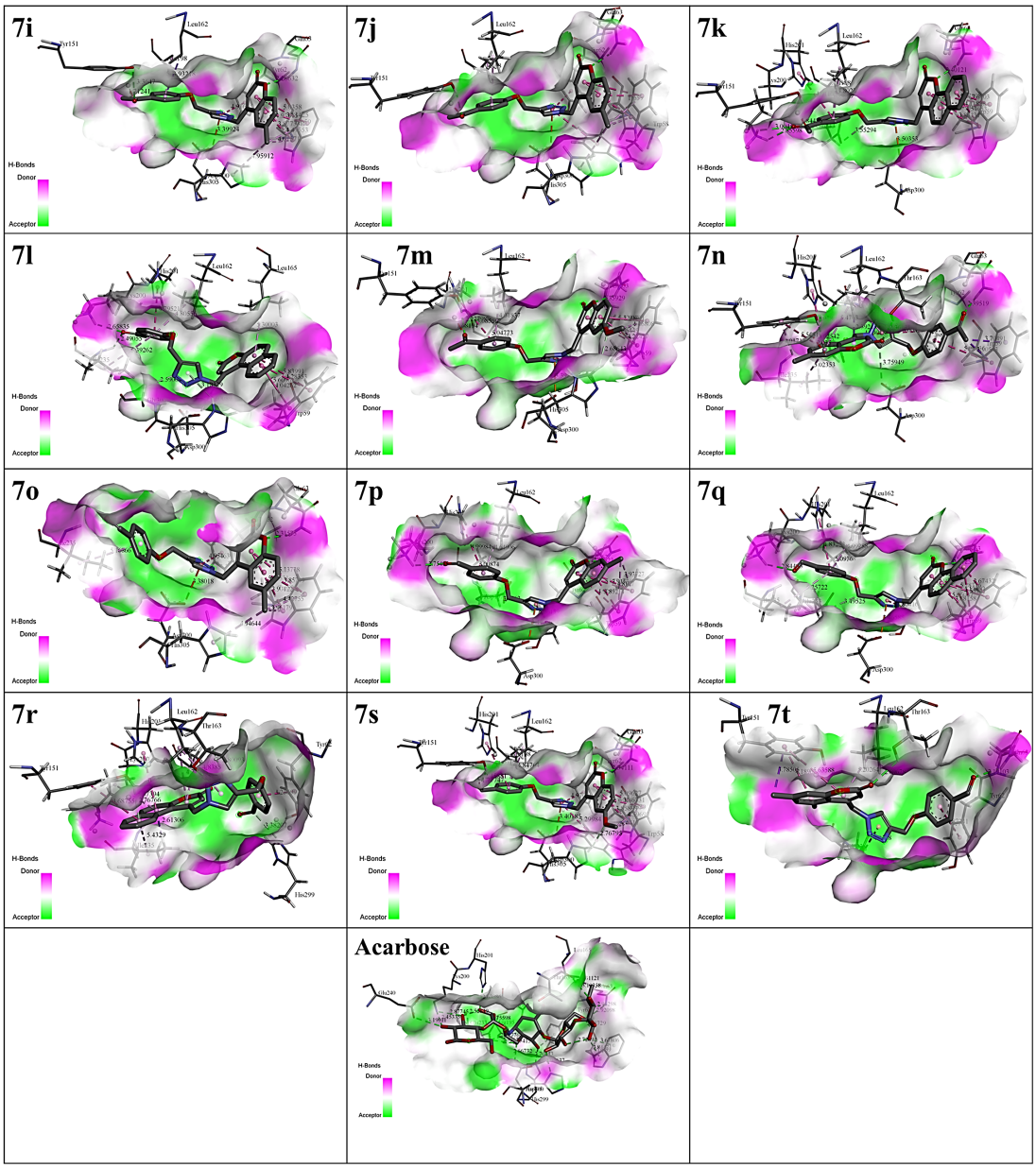

Figure 3. 3D interactions of the best binding modes with the least binding energy of newly synthesized compounds 7i-t at the active site pocket of the enzyme human pancreatic α-amylase (1B2Y).

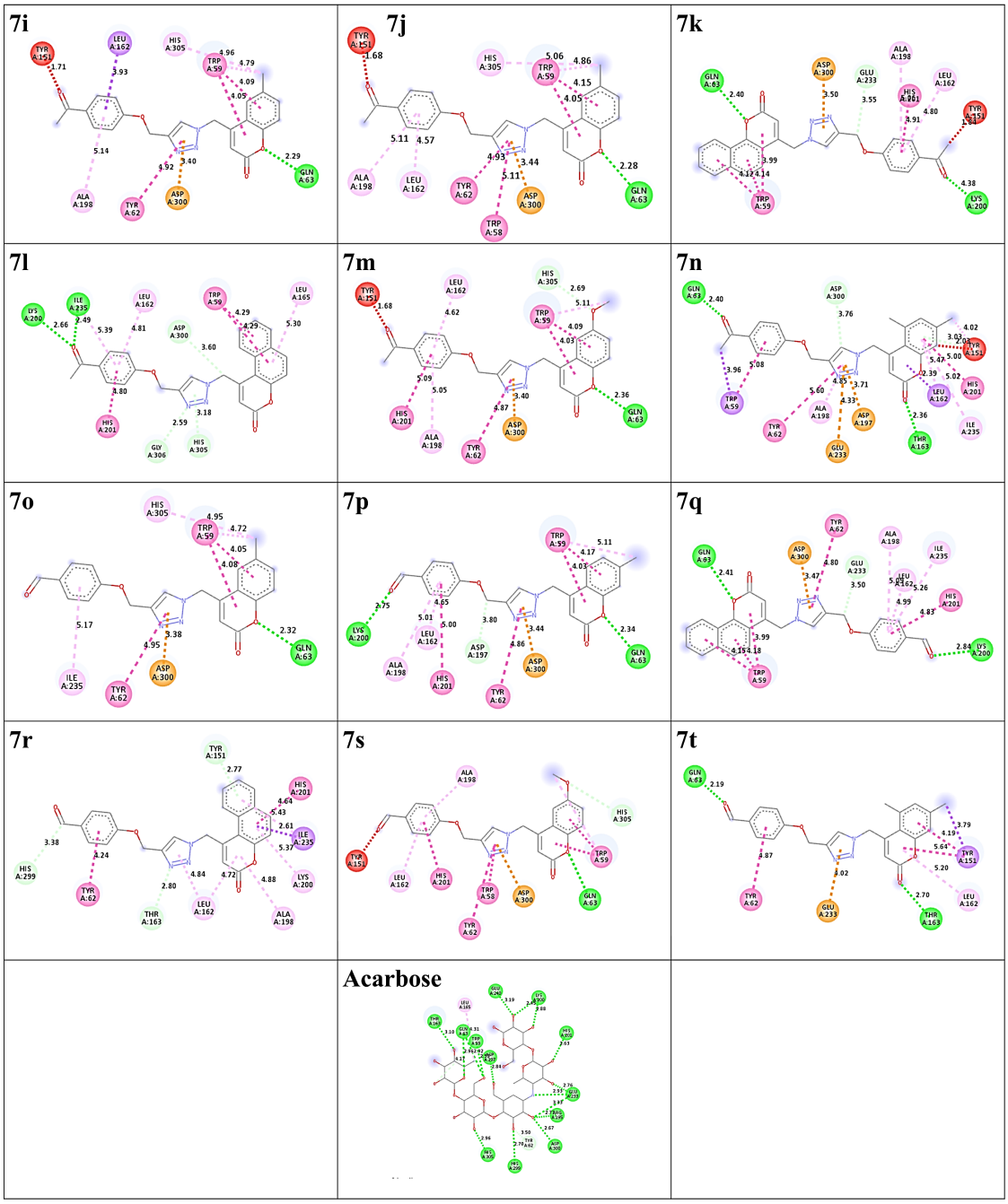

Figure 4. 2D diagram showing the interactions of the best binding modes of newly synthesized compounds **7(i-t)** at the active site of the enzyme human pancreatic α-amylase (1B2Y).

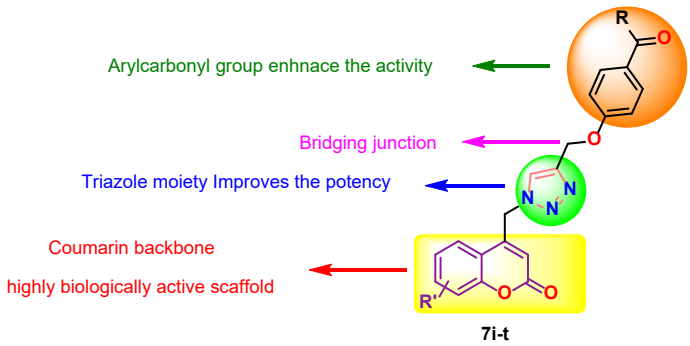

Figure 5. Representation of structure-activity relationship of synthesized compounds for biological activity.

in enhanced anti-inflammatory behaviour compared to the substitution of methoxy 7s and dimethyl 7t in keto derivatives. Overall, it can be concluded that 7o, p, q, r was shown to be more effective anti-inflammatory activity by showing lower IC_{50} values than the standard drug diclofenac.

The relevance of coumarin, traizole and arylcarbonyl moieties in the synthesised compounds for α-amylase inhibition has been well validated by docking studies, which have revealed numerous strong interactions inside the active site of the amylase protein. The coumarin moiety's ring oxygen formed strong hydrogen bonds with the GLN 63 residue, but the aromatic ring exhibited π-π stacking interactions with TRP 59 residue. The methyl, methoxy and benzo substitutions on coumarin resulted in additional π-alkyl, hydrogen, and pi-pi stacked interactions, respectively. The triazole moiety exhibited π-anion electrostatic contact with ASP 300, π-π T-shaped interaction with TYR 62, and additional scattering interactions that improved Trp 59. The superior activity of keto derivatives is supported by a strong hydrogen bonding of the keto group with protein residues TYR 151, which are absent in their respective aldehydic counterparts. General observation of the structure-activity relationship of the synthesized compounds as depicted (Figure 5).

5. Conclusions

In summary, a series of novel 1,2,3-(triazol-4-yl)-2*H*-chromen-2-ones were synthesized and characterized using contemporary spectroscopic approaches. Furthermore, compared to the IC_{50} value of the standard drug acarbose, all compounds synthesized have shown an outstanding *in vitro* antihyperglycemic action with two to five times higher IC_{50} values in α-amylase and α-glucosidase inhibition assays compared to standard acarbose. Among the synthesized hybrids, compound 7l exhibited an outstanding α-amylase and α-glucosidase inhibitory potential, with IC_{50} values of 0.67±0.014 mg/mL and 0.72±0.012 mg/mL in addition to that compound 7o has exhibited the best anti-inflammatory activity with IC_{50} values of 0.54±0.003 mg/mL. Furthermore, molecular docking studies have substantiated the presence of strong molecular interaction synthesising hybrids with binding sites of human pancreatic α-amylase (PDB ID: 1B2Y) than that of a conventional ligand acarbose with an effective binding energy of -9.0 to -10.6 kcal/mol. Our novel effort to incorporate aromatic carbonyl in the coumarin-triazole scaffold has resulted in better antidiabetic potency compared to the existing library of coumarin derivatives in the literature. Since the synthesized compound 7l has shown excellent antihyperglycemic activity, it can be evaluated for use as a lead drug in an antidiabetic drug development program.

Acknowledgements

One of the authors, Vinayaka Chandrappa Barangi, acknowledges the University's Grant Commission for providing Council of Scientific and Industrial Research-University Grant Commission (CSIR-UGC) fellowship (Ref. No.: 151674 Roll. No. DEC: 2018-2019). The authors also thank the University Scientific Instrumentation centre (USIC) and the Sophisticated Analytical Instrument Facilities-Department of Science and Technology (SAIF-DST) of Karnatak University, Dharwad, India for spectral analyses. The authors also thank Karnatak University, Dharwad, India for financial support as seed grant for the research program.

Disclosure statement

Conflict of interest: The authors declare that they have no conflict of interest.
Ethical approval: All ethical guidelines have been adhered.
Sample availability: Samples of the compounds are available from the author.

CRediT authorship contribution statement

Conceptualization: Lokesh Anand Shastri, Vinayaka Chandrappa Barangi; Methodology: Vinayaka Chandrappa Barangi; Software: Nagarjuna Prakash Dalbanjan; Validation: Vinay Sunagar; Formal Analysis: Delicia Avilla Barretto; Investigation: Lokesh Anand Shastri; Resources: Rohini Sangappanavar, Karhik Inamdar; Data Curation: Prakasha Kothathi Chowdegowda; Writing - Original Draft: Vinayaka Chandrappa Barangi; Writing - Review and Editing: Lokesh Anand Shastri; Visualization: Prakasha Kothathi Chowdegowda; Supervision: Lokesh Anand Shastri.

ORCID and Email

Vinayaka Chandrappa Barangi
vcbarangi41@gmail.com
https://orcid.org/0009-0004-9918-0570
Lokesh Anand Shastri
drlashastri@kud.ac.in
https://orcid.org/0000-0002-5672-8442
Prakasha Kothathi Chowdegowda
dr.kcprakash@gmail.com
https://orcid.org/0000-0003-4888-4434
Rohini Sangappanavar
rbsangappanavar@gmail.com
https://orcid.org/0009-0008-2170-4038
Karthik Inamdar
karthikrinamdar151947@gmail.com
https://orcid.org/0009-0004-9947-136X
Nagarjuna Prakash Dalbanjan
dnp.biochem@gmail.com
https://orcid.org/0000-0003-1053-6610
Delicia Avillia Barretto
delicia@unigoa.ac.in
https://orcid.org/0000-0001-9122-0663
Vinay Sunagar
vinaysunagar@gssbgm.edu.in
https://orcid.org/0000-0001-9804-7330

References

[1]. Soni, R.; Durgapal, S. D.; Soman, S. S.; Georrge, J. J. Design, synthesis and anti-diabetic activity of chromen-2-one derivatives. *Arab. J. Chem.* **2019**, *12*, 701–708.
[2]. Powell, H. C.; Mizisin, A. P. Diabetic neuropathy. In *Encyclopedia of Neuroscience*; Elsevier, 2009; pp. 511–516.
[3]. Kropp, M.; Golubnitschaja, O.; Mazurakova, A.; Koklesova, L.; Sargheini, N.; Vo, T.-T. K. S.; de Clerck, E.; Polivka, J., Jr; Potuznik, P.; Polivka, J.; Stetkarova, I.; Kubatka, P.; Thumann, G. Diabetic retinopathy as the leading cause of blindness and early predictor of cascading complications—risks and mitigation. *EPMA J.* **2023**, *14*, 21–42.
[4]. Said, G. Diabetic neuropathy. In *Handbook of Clinical Neurology*; Elsevier, 2013; pp. 579–589.
[5]. Ranđelović, S.; Bipat, R. A review of coumarins and coumarin-related compounds for their potential antidiabetic effect. *Clin. Med. Insights Endocrinol. Diabetes* **2021**, *14*, 117955142110420.
[6]. Li, H.; Yao, Y.; Li, L. Coumarins as potential antidiabetic agents. *J. Pharm. Pharmacol.* **2017**, *69*, 1253–1264.
[7]. Pan, Y.; Liu, T.; Wang, X.; Sun, J. Research progress of coumarins and their derivatives in the treatment of diabetes. *J. Enzyme Inhib. Med. Chem.* **2022**, *37*, 616–628.
[8]. Jadhav, P. B.; Jadhav, S. B.; Zehravi, M.; Mubarak, M. S.; Islam, F.; Jeandet, P.; Khan, S. L.; Hossain, N.; Rashid, S.; Ming, L. C.; Sarker, M. M. R.; Azlina, M. F. N. Virtual screening, synthesis, and biological evaluation of some carbohydrazide derivatives as potential DPP-IV inhibitors. *Molecules* **2022**, *28*, 149.
[9]. Lon, H.-K.; Liu, D.; Jusko, W. J. Pharmacokinetic/pharmacodynamic modeling in inflammation. *Crit. Rev. Biomed. Eng.* **2012**, *40*, 295–312.
[10]. Maritim, A. C.; Sanders, R. A.; Watkins, J. B., III Diabetes, oxidative stress, and antioxidants: A review. *J. Biochem. Mol. Toxicol.* **2003**, *17*, 24–38.
[11]. Ferreira, S. H.; Vane, J. R. New aspects of the mode of action of nonsteroid anti-inflammatory drugs. *Annu. Rev. Pharmacol.* **1974**, *14*, 57–73.

[12]. Kamat, V.; Santosh, R.; Poojary, B.; Nayak, S. P.; Kumar, B. K.; Sankaranarayanan, M.; Faheem; Khanapure, S.; Barretto, D. A.; Vootla, S. K. Pyridine- and thiazole-based hydrazides with promising anti-inflammatory and antimicrobial activities along with their *in silico* studies. *ACS Omega* **2020**, *5*, 25228–25239.
[13]. Tiwari, A. D.; Panda, S. S.; Girgis, A. S.; Sahu, S.; George, R. F.; Srour, A. M.; Starza, B. L.; Asiri, A. M.; Hall, C. D.; Katritzky, A. R. Microwave assisted synthesis and QSAR study of novel NSAID acetaminophen conjugates with amino acid linkers. *Org. Biomol. Chem.* **2014**, *12*, 7238–7249.
[14]. Channa Basappa, V.; Hamse Kameshwar, V.; Kumara, K.; Achutha, D. K.; Neratur Krishnappagowda, L.; Kariyappa, A. K. Design and synthesis of coumarin-triazole hybrids: biocompatible anti-diabetic agents, in silico molecular docking and ADME screening. *Heliyon* **2020**, *6*, e05290.
[15]. Ostrowska, K. Coumarin-piperazine derivatives as biologically active compounds. *Saudi Pharm. J.* **2020**, *28*, 220–232.
[16]. Abdel-Kader, N. S.; Moustafa, H.; El-Ansary, A. L.; Farghaly, A. M. Theoretical calculations for new coumarin Schiff base complexes as candidates for in vitro and in silico biological applications. *Appl. Organomet. Chem.* **2022**, *36*, e6840.
[17]. El-Sherief, H. A.; Abuo-Rahma, G. E.-D. A.; Shoman, M. E.; Beshr, E. A.; Abdel-baky, R. M. Design and synthesis of new coumarin–chalcone/NO hybrids of potential biological activity. *Med. Chem. Res.* **2017**, *26*, 3077–3090.
[18]. Durgapal, S. D.; Soman, S. S. Evaluation of novel coumarin-proline sulfonamide hybrids as anticancer and antidiabetic agents. *Synth. Commun.* **2019**, 1–15.
[19]. Emam, S. H.; Sonousi, A.; Osman, E. O.; Hwang, D.; Kim, G.-D.; Hassan, R. A. Design and synthesis of methoxyphenyl- and coumarin-based chalcone derivatives as anti-inflammatory agents by inhibition of NO production and down-regulation of NF-κB in LPS-induced RAW264.7 macrophage cells. *Bioorg. Chem.* **2021**, *107*, 104630.
[20]. Gudimani, P.; Shastri, S. L.; Pawar, V.; Hebbar, N. U.; Shastri, L. A.; Joshi, S.; Vootla, S. K.; Khanapure, S.; Sunagar, V. Synthesis, molecular docking, and biological evaluation of methyl-5-(hydroxyimino)-3-(aryl-substituted)hexanoate derivatives. *Eur. J. Chem.* **2022**, *13*, 151–161.
[21]. Alshibl, H. M.; Al-Abdullah, E. S.; Haiba, M. E.; Alkahtani, H. M.; Awad, G. E. A.; Mahmoud, A. H.; Ibrahim, B. M. M.; Bari, A.; Villinger, A. Synthesis and evaluation of new coumarin derivatives as antioxidant, antimicrobial, and anti-inflammatory agents. *Molecules* **2020**, *25*, 3251.
[22]. Tapanyiğit, O.; Demirkol, O.; Güler, E.; Erşatır, M.; Çam, M. E.; Giray, E. S. Synthesis and investigation of anti-inflammatory and anticonvulsant activities of novel coumarin-diacylated hydrazide derivatives. *Arab. J. Chem.* **2020**, *13*, 9105–9117.
[23]. Bhagat, K.; Bhagat, J.; Gupta, M. K.; Singh, J. V.; Gulati, H. K.; Singh, A.; Kaur, K.; Kaur, G.; Sharma, S.; Rana, A.; Singh, H.; Sharma, S.; Singh Bedi, P. M. Design, synthesis, antimicrobial evaluation, and molecular modeling studies of novel indolinedione–coumarin molecular hybrids. *ACS Omega* **2019**, *4*, 8720–8730.
[24]. Puthran, D.; Kamat, V.; Purushotham, N.; Poojary, B.; Rasheed, M. S.; Hegde, H. Expeditious synthesis and biological evaluation of pyrazole conjugated selenium Lumefantrine analogues. *J. Iran. Chem. Soc.* **2023**, *20*, 1903–1916.
[25]. Hwu, J. R.; Kapoor, M.; Gupta, N. K.; Tsay, S.-C.; Huang, W.-C.; Tan, K.-T.; Hu, Y.-C.; Lyssen, P.; Neyts, J. Synthesis and antiviral activities of quinazolinamine–coumarin conjugates toward chikungunya and hepatitis C viruses. *Eur. J. Med. Chem.* **2022**, *232*, 114164.
[26]. Medina, F. G.; Marrero, J. G.; Macías-Alonso, M.; González, M. C.; Córdova-Guerrero, I.; Teissier García, A. G.; Osegueda-Robles, S. Coumarin heterocyclic derivatives: chemical synthesis and biological activity. *Nat. Prod. Rep.* **2015**, *32*, 1472–1507.
[27]. Anand, A.; Naik, R. J.; Revankar, H. M.; Kulkarni, M. V.; Dixit, S. R.; Joshi, S. D. A click chemistry approach for the synthesis of mono and bis aryloxy linked coumarinyl triazoles as anti-tubercular agents. *Eur. J. Med. Chem.* **2015**, *105*, 194–207.
[28]. Hebbar, N. U.; Patil, A. R.; Gudimani, P.; Shastri, S. L.; Shastri, L. A.; Joshi, S. D.; Vootla, S. K.; Khanapure, S.; Shettar, A. K.; Sungar, V. A. Click approach for synthesis of 3,4-dihydro-2(1H) quinolinone, coumarin moored 1,2,3-triazoles as inhibitor of mycobacteria tuberculosis H37RV, their antioxidant, cytotoxicity and in-silico studies. *J. Mol. Struct.* **2022**, *1269*, 133795.
[29]. Kharb, R.; Sharma, P. C.; Yar, M. S. Pharmacological significance of triazole scaffold. *J. Enzyme Inhib. Med. Chem.* **2011**, *26*, 1–21.
[30]. Metre, T. V.; Kodasi, B.; Bayannavar, P. K.; Bheemayya, L.; Nadoni, V. B.; Hoolageri, S. R.; Shettar, A. K.; Joshi, S. D.; Kumbar, V. M.; Kamble, R. R. Coumarin-4-yl-1,2,3-triazol-4-yl-methyl-thiazolidine-2,4-diones: Synthesis, glucose uptake activity and cytotoxic evaluation. *Bioorg. Chem.* **2023**, *130*, 106235.
[31]. Susmita Rayawgol, B.; Sujatha, K.; Dalbanjan, N. P.; Praveen Kumar, S. K.; Rajappa, S. K. Development of novel, green, efficient approach for the synthesis of indazole and its derivatives; insights into their pharmacological and molecular docking studies. *J. Indian Chem. Soc.* **2024**, *101*, 101178.
[32]. Hameed, S.; Kanwal; Seraj, F.; Rafique, R.; Chigurupati, S.; Wadood, A.; Rehman, A. U.; Venugopal, V.; Salar, U.; Taha, M.; Khan, K. M. Synthesis of benzotriazoles derivatives and their dual potential as α-amylase and α-glucosidase inhibitors in vitro: Structure-activity relationship, molecular docking, and kinetic studies. *Eur. J. Med. Chem.* **2019**, *183*, 111677.
[33]. Sun, H.; Song, X.; Tao, Y.; Li, M.; Yang, K.; Zheng, H.; Jin, Z.; Dodd, R. H.; Pan, G.; Lu, K.; Yu, P. Synthesis & α-glucosidase inhibitory & glucose consumption-promoting activities of flavonoid–coumarin hybrids. *Future Med. Chem.* **2018**, *10*, 1055–1066.
[34]. Bak, E.-J.; Park, H.-G.; Lee, C.-H.; Lee, T.-I.; Woo, G.-H.; Na, Y.-H.; Yoo, Y.-J.; Cha, J.-H. Effects of novel chalcone derivatives on α-glucosidase, dipeptidyl peptidase-4, and adipocyte differentiation in vitro. *BMB Rep.* **2011**, *44*, 410–414.
[35]. Asgari, M. S.; Mohammadi-Khanaposhtani, M.; Kiani, M.; Ranjbar, P. R.; Zabihi, E.; Pourbagher, R.; Rahimi, R.; Faramarzi, M. A.; Biglar, M.; Larijani, B.; Mahdavi, M.; Hamedifar, H.; Hajimiri, M. H. Biscoumarin-1,2,3-triazole hybrids as novel anti-diabetic agents: Design, synthesis, in vitro α-glucosidase inhibition, kinetic, and docking studies. *Bioorg. Chem.* **2019**, *92*, 103206.
[36]. Bansal, Y.; Sethi, P.; Bansal, G. Coumarin: a potential nucleus for anti-inflammatory molecules. *Med. Chem. Res.* **2013**, *22*, 3049–3060.
[37]. Dharavath, R.; Nagaraju, N.; Reddy, M. R.; Ashok, D.; Sarasija, M.; Vijjulatha, M.; Vani; Jyothi, K.; Prashanthi, G. Microwave-assisted synthesis, biological evaluation and molecular docking studies of new coumarin-based 1,2,3-triazoles. *RSC Adv.* **2020**, *10*, 11615–11623.
[38]. Musa, A.; Abulkhair, H. S.; Aljuhani, A.; Rezki, N.; Abdelgawad, M. A.; Shalaby, K.; El-Ghorab, A. H.; Aouad, M. R. Phenylpyrazolone-1,2,3-triazole hybrids as potent antiviral agents with promising SARS-CoV-2 Main protease inhibition potential. *Pharmaceuticals (Basel)* **2023**, *16*, 463.
[39]. Kumar, V.; Lal, K.; Kumar, A.; Tittal, R. K.; Singh, M. B.; Singh, P. Efficient synthesis, antimicrobial and molecular modelling studies of 3-sulfenylated oxindole linked 1,2,3-triazole hybrids. *Res. Chem. Intermed.* **2023**, *49*, 917–937.
[40]. Manzoor, S.; Almarghalani, D. A.; James, A. W.; Raza, M. K.; Kausar, T.; Nayeem, S. M.; Hoda, N.; Shah, Z. A. Synthesis and pharmacological evaluation of novel triazole-pyrimidine hybrids as potential neuroprotective and anti-neuroinflammatory agents. *Pharm. Res.* **2023**, *40*, 167–185.
[41]. Al-Ghulikah, H.; Ghabi, A.; Haouas, A.; Mtiraoui, H.; Jeanneau, E.; Msaddek, M. Synthesis of new 1,2,3-triazole linked benzimidazolidinone: Single crystal X-ray structure, biological activities evaluation and molecular docking studies. *Arab. J. Chem.* **2023**, *16*, 104566.
[42]. Kapkoti, D. S.; Kumar, S.; Kumar, A.; Darokar, M. P.; Pal, A.; Bhakuni, R. S. Design and synthesis of novel glycyrrhetinic acid-triazole derivatives that exert anti-plasmodial activity inducing mitochondrial-dependent apoptosis in *Plasmodium falciparum*. *New J Chem* **2023**, *47*, 6967–6982.
[43]. Shafique, K.; Farrukh, A.; Mahmood Ali, T.; Qasim, S.; Jafri, L.; Abd-Rabboh, H. S. M.; AL-Anazy, M. M.; Kalsoom, S. Designing click one-pot synthesis and antidiabetic studies of 1,2,3-triazole derivatives. *Molecules* **2023**, *28*, 3104.
[44]. Sireesha, R.; Tej, M. B.; Poojith, N.; Sreenivasulu, R.; Musuluri, M.; Subbarao, M. Synthesis of substituted aryl incorporated oxazolo[4,5-b]pyridine-triazole derivatives: Anticancer evaluation and molecular docking studies. *Polycycl. Aromat. Compd.* **2023**, *43*, 915–932.
[45]. Khouzani, M. A.; Mogharabi, M.; Faramarzi, M. A.; Mojtabavi, S.; Azizian, H.; Mahdavi, M.; Hashemi, S. M. Development of coumarin tagged 1,2,3-triazole derivatives targeting α-glucosidase inhibition: Synthetic modification, biological evaluation, kinetic and in silico studies. *J. Mol. Struct.* **2023**, *1282*, 135194.
[46]. Zala, A. R.; Naik, H. N.; Ahmad, I.; Patel, H.; Jauhari, S.; Kumari, P. Design and synthesis of novel 1,2,3-triazole linked hybrids: Molecular docking, MD simulation, and their antidiabetic efficacy as α-Amylase inhibitors. *J. Mol. Struct.* **2023**, *1285*, 135493.
[47]. Channabasappa, V.; Kumara, K.; Kariyappa, A. K. Design, synthesis of coumarin tethered 1,2,3-triazoles analogues, evaluation of their antimicrobial and α-amylase inhibition activities. *J. Chem. Sci. (Bangalore)* **2021**, *133*.
[48]. Sharma, A.; Bharate, S. B. Synthesis and biological evaluation of coumarin triazoles as dual inhibitors of cholinesterases and β-secretase. *ACS Omega* **2023**, *8*, 11161–11176.
[49]. Design, Synthesis, Anticancer Activity and Molecular Docking of New 1,2,3-Triazole combined Glucosides with coumarin. *Journal of Population Therapeutics and Clinical Pharmacology* **2023**, *30*, 345–356.
[50]. Singh, G.; Mohit; Diksha; Suman; Priyanka; Singh, K. N.; Gonzalez-Silvera, D.; Espinosa-Ruiz, C.; Esteban, M. A. Functionalized organosilanes and their magnetic nanoparticles as receptor for Sn (II) ions detection and potent antioxidants. *J. Mol. Struct.* **2022**, *1247*, 131297.

[51]. Kusanur, R. A.; Kulkarni, M. V.; Kulkarni, G. M.; Nayak, S. K.; Guru Row, T. N.; Ganesan, K.; Sun, C.-M. Unusual anisotropic effects from 1,3-dipolar cycloadducts of 4-azidomethyl coumarins. *J. Heterocycl. Chem.* **2010**, *47*, 91–97.
[52]. Pereira, R. P.; Jadhav, R.; Baghela, A.; Barretto, D. A. In vitro assessment of probiotic potential of Saccharomyces cerevisiae DABRP5 isolated from Bollo batter, a traditional goan fermented food. *Probiotics Antimicrob. Proteins* **2021**, *13*, 796–808.
[53]. Granados-Guzmán, G.; Castro-Rios, R.; de Torres, N. W.; Salazar-Aranda, R. Optimization and validation of a microscale in vitro method to assess α-glucosidase inhibition activity. *Curr. Anal. Chem.* **2018**, *14*, 458–464.
[54]. Mizushima, Y.; Kobayashi, M. Interaction of anti-inflammatory drugs with serum proteins, especially with some biologically active proteins. *J. Pharm. Pharmacol.* **2011**, *20*, 169–173.
[55]. Sakat, S.; Tupe, P.; Juvekar, A. Gastroprotective effect of methanol extract of Oxalis corniculata Linn (whole plant) experimental animals. *Planta Med.* **2010**, *76*.
[56]. Morris, G. M.; Huey, R.; Lindstrom, W.; Sanner, M. F.; Belew, R. K.; Goodsell, D. S.; Olson, A. J. AutoDock4 and AutoDockTools4: Automated docking with selective receptor flexibility. *J. Comput. Chem.* **2009**, *30*, 2785–2791.
[57]. Trott, O.; Olson, A. J. AutoDock Vina: Improving the speed and accuracy of docking with a new scoring function, efficient optimization, and multithreading. *J. Comput. Chem.* **2010**, *31*, 455–461.
[58]. O'Boyle, N. M. Towards a Universal SMILES representation - A standard method to generate canonical SMILES based on the InChI. *J. Cheminform.* **2012**, *4*.
[59]. Ambrus, G.; Whitby, L. R.; Singer, E. L.; Trott, O.; Choi, E.; Olson, A. J.; Boger, D. L.; Gerace, L. Small molecule peptidomimetic inhibitors of importin α/β mediated nuclear transport. *Bioorg. Med. Chem.* **2010**, *18*, 7611–7620.
[60]. Feunaing, R. T.; Tamfu, A. N.; Gbaweng, A. J. Y.; Mekontso Magnibou, L.; Ntchapda, F.; Henoumont, C.; Laurent, S.; Talla, E.; Dinica, R. M. In Vitro Evaluation of α-amylase and α-glucosidase Inhibition of 2,3-Epoxyprocyanidin C1 and Other Constituents from Pterocarpus erinaceus Poir. *Molecules* **2022**, *28*, 126.
[61]. Kamat, V.; Barretto, D. A.; Poojary, B.; Kumar, A.; Patil, V. B.; Hamzad, S. In vitro α-amylase and α-glucosidase inhibition study of dihydropyrimidinones synthesized via one-pot Biginelli reaction in the presence of a green catalyst. *Bioorg. Chem.* **2024**, *143*, 107085.
[62]. Xie, Z.; Wang, G.; Wang, J.; Chen, M.; Peng, Y.; Li, L.; Deng, B.; Chen, S.; Li, W. Synthesis, biological evaluation, and molecular docking studies of novel isatin-thiazole derivatives as α-glucosidase inhibitors. *Molecules* **2017**, *22*, 659.